New Jersey Institute of Technology
Digital Commons @ NJIT

Dissertations | Theses and Dissertations

Spring 2004

A Gibbs sampling approach to maximum a posteriori time delay and amplitude estimations

Michele Picarelli
New Jersey Institute of Technology

Follow this and additional works at: https://digitalcommons.njit.edu/dissertations

 Part of the Mathematics Commons

Recommended Citation
Picarelli, Michele, "A Gibbs sampling approach to maximum a posteriori time delay and amplitude estimations" (2004). *Dissertations*. 637.
https://digitalcommons.njit.edu/dissertations/637

This Dissertation is brought to you for free and open access by the Theses and Dissertations at Digital Commons @ NJIT. It has been accepted for inclusion in Dissertations by an authorized administrator of Digital Commons @ NJIT. For more information, please contact digitalcommons@njit.edu.

Copyright Warning & Restrictions

The copyright law of the United States (Title 17, United States Code) governs the making of photocopies or other reproductions of copyrighted material.

Under certain conditions specified in the law, libraries and archives are authorized to furnish a photocopy or other reproduction. One of these specified conditions is that the photocopy or reproduction is not to be "used for any purpose other than private study, scholarship, or research." If a, user makes a request for, or later uses, a photocopy or reproduction for purposes in excess of "fair use" that user may be liable for copyright infringement,

This institution reserves the right to refuse to accept a copying order if, in its judgment, fulfillment of the order would involve violation of copyright law.

Please Note: The author retains the copyright while the New Jersey Institute of Technology reserves the right to distribute this thesis or dissertation

Printing note: If you do not wish to print this page, then select "Pages from: first page # to: last page #" on the print dialog screen

The Van Houten library has removed some of the personal information and all signatures from the approval page and biographical sketches of theses and dissertations in order to protect the identity of NJIT graduates and faculty.

ABSTRACT

A GIBBS SAMPLING APPROACH TO MAXIMUM A POSTERIORI TIME DELAY AND AMPLITUDE ESTIMATION

by
Michele Picarelli

Research concerned with underwater propagation in a shallow ocean environment is a growing area of study. In particular, the development of fast and accurate computational methods to estimate environmental parameters and source location is desired. In this work, only select features of the acoustic field are investigated, namely, the time delays and amplitudes of individual paths, the signal-to-noise ratio, and the number of multi-path arrivals. The amplitudes and delays contain pertinent information about the geometry associated with the environment of interest. Estimating the time delays and amplitudes of select paths in a manner that is both accurate and time efficient, however, is not a trivial task. A Gibbs Sampling Monte Carlo technique is proposed to recover these arrivals and their features. The method is tested on synthetic data as well as data from the Haro Straight experiment for the estimation of the number of arrivals, the amplitude and time delay associated with each arrival, and the variance of noise. Signals involved in shallow water propagation closely resemble signals obtained in other areas such as radar and communication problems. Therefore, the estimation techniques presented here may be useful in these, among several other, applications.

A GIBBS SAMPLING APPROACH TO MAXIMUM A POSTERIORI TIME DELAY AND AMPLITUDE ESTIMATION

by
Michele Picarelli

A Dissertation
Submitted to the Faculty of
New Jersey Institute of Technology and
Rutgers, The State University of New Jersey – Newark
in Partial Fulfillment of the Requirements for the Degree of
Doctor of Philosophy in Mathematical Sciences

Department of Mathematical Sciences, NJIT
Department of Mathematics and Computer Science, Rutgers-Newark

May 2004

Copyright © 2004 by Michele Picarelli

ALL RIGHTS RESERVED

APPROVAL PAGE

A GIBBS SAMPLING APPROACH TO MAXIMUM A POSTERIORI TIME DELAY AND AMPLITUDE ESTIMATION

Michele Picarelli

Dr. Zoi-Heleni Michalopoulou, Dissertation Advisor — Date
Associate Professor of Mathematical Sciences and of Electrical and Computer Engineering, NJIT

Dr. Daljit S. Ahluwalia, Committee Member — Date
Professor of Mathematical Sciences, NJIT

Dr. John K. Bechtold, Committee Member — Date
Associate Professor of Mathematical Sciences, NJIT

Dr. Manish C. Bhattacharjee, Committee Member — Date
Professor of Mathematical Sciences, NJIT

Dr. Alexander M. Haimovich, Committee Member — Date
Professor of Electrical and Computer Engineering, NJIT

BIOGRAPHICAL SKETCH

Author: Michele Picarelli

Degree: Doctor of Philosophy

Date: May 2004

Undergraduate and Graduate Education:

- Doctor of Philosophy in Mathematical Sciences,
  New Jersey Institute of Technology, Newark, NJ, 2004
- Master of Science in Applied Mathematics,
  New Jersey Institute of Technology, Newark, NJ, 1998
- Bachelor of Science in Mathematics,
  St. Peter's College, Jersey City, NJ, 1996

Major: Mathematical Sciences

Presentations and Publications:

Z. Michalopoulou and M. Picarelli
"A Gibbs Sampling Approach To Maximum A Posteriori Time Delay And Amplitude Estimation,"
2002 IEEE International Conference on Acoustics, Speech and Signal Processing, vol. 3, pp. 3001-3004, 2002.

Z. Michalopoulou, X. Ma, M. Picarelli and U. Ghosh-Dastidar,
"Fast Matching Methods for Inversion with Underwater Sound,"
OCEANS 2000 MTS/IEEE Conference and Exhibition, vol. 1, pp. 647-651, 2000.

Z. Michalopoulou and M. Picarelli,
"A Gibbs Sampling Approach To Maximum A Posteriori Time Delay And Amplitude Estimation,"
Invited Lecture, Nashville, Tennessee, 2003.

Z. Michalopoulou and M. Picarelli,
"Gibbs Sampling For Time Delay And Amplitude Estimation In An Uncertain Environment,"
Poster Presentation, Orlando, Florida, 2002.

To my mother, without whom this would not have been possible. Thank you for always supporting me, believing in me and loving me unconditionally. Everything I am is because of you, "the wind beneath my wings".

ACKNOWLEDGMENT

I would like to thank Dr. Zoi-Heleni Michalopoulou for being the best graduate advisor a student could ask for. I have said many times, "I did not pick a research topic, I picked a research advisor." and now it is my privilege and honor to thank her in writing. Often brilliant people are consumed with their research and impatient with those whom are not at their level. Dr. Michalopoulou is the exception. In addition, I would like to thank the members of my committee, Dr. Daljit S. Ahluwalia, Dr. Manish C. Bhattacharjee, Dr. John K. Bechtold, and Dr. Alexander M. Haimovich for their time and most valuable input on this research project. I would also like to thank the ONR Ocean Acoustics for the grants that helped fund most of this research project. Finally, I would like to thank the mathematics department at NJIT for both their financial support and for the opportunity to grow professionally.

TABLE OF CONTENTS

TABLE OF CONTENTS
(Continued)

Chapter **Page**

LIST OF TABLES

LIST OF TABLES
(Continued)

Table **Page**

LIST OF TABLES
(Continued)

Table **Page**

LIST OF FIGURES

LIST OF FIGURES
(Continued)

Figure **Page**

LIST OF FIGURES
(Continued)

Figure **Page**

CHAPTER 1

INTRODUCTION

1.1 Motivation

In the last few decades, there has been explosive growth in the development of numerical models used as tools in research involving underwater acoustics. One particular area of interest in underwater acoustics is the propagation of sound in a shallow ocean environment. The reason, in part, for such interest is the way submarines are constructed today. First, some submarines, such as those which transport navy seals, are much smaller than they were years ago. Their compact size now allows the submarines to maneuver into more shallow water. Second, the submarines are designed to be much quieter than they were in the past. This makes them more difficult to detect. The harder these sounds are to detect, the easier it is for these vessels to approach land, and hence, travel into shallow water. These sounds, if detected, can be linked to a sound propagation model for the estimation of source location.

Difficulties arise when one attempts to predict propagation of sound in a shallow water ocean environment. The difficulty stems from the fact that a signal travelling in shallow water will interact multiple times with both the ocean's surface and bottom. In addition to knowing the source location and receiver location, as well as the properties of the water, such as sound speed and depth of the water column, we also need information about the parameters associated with the ocean bottom. We need to identify the layers of the ocean bottom that the transmitted signal has interacted with and how this interaction affects the received signal. Then, for each layer in the bottom, we need to know the sound speed, density, attenuation and thickness of the sediment. Thus, there has been strong motivation for the development of fast and

accurate inversion models for the concurrent estimation of location and environmental parameters. In [1, 2, 3, 4, 5] it was shown that linking arrival times and amplitudes of received time series to acoustic models, we can extract valuable information on the environment and the location of the sound emitting source. However, accurate identification of arrival times and amplitudes is not always simple. This identification is the focus of this work.

1.2 Environment

We are interested in modelling sound phenomena generated by a source and received by a hydrophone in a range-independent shallow water ocean environment. In shallow water, signals transmitted from an acoustic source usually arrive at the receiver through multi-path propagation. Figure 1.1 shows three typical paths the rays will take in travelling from the source to the receiver; there is a ray that goes directly from the source to the receiver, a ray that is reflected off the ocean surface, and a ray that is reflected off the ocean bottom before they reach the receiver.

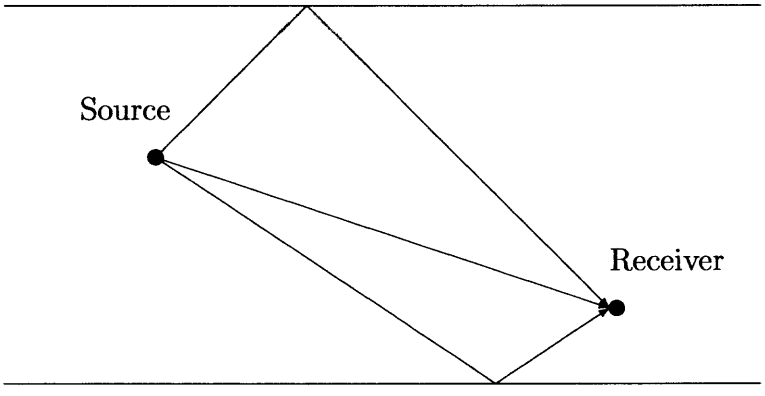

Figure 1.1 Typical ray paths.

Thus the received signal in a shallow water environment, as well as in many other problems in signal processing, can be modelled as a superposition of a finite number of signals embedded in noise. These signals consist of delayed and attenuated replicas of the transmitted signal due to various interactions with the boundaries. The

received signal can be generally written as:

$$r(n) = \sum_{i=1}^{M} a_i s(n - n_i) + w(n). \tag{1.1}$$

M is the number of arrivals, a_i and n_i are the amplitude and time delay of the ith arrival, and $w(n)$ is additive noise.

Figure 1.2 captures some of the features associated with arrivals corresponding to distinct paths. This figure, however, is an over-simplification of an actual signal obtained at a receiver because it does not include noise and it reflects the case of undistorted high frequency signals.

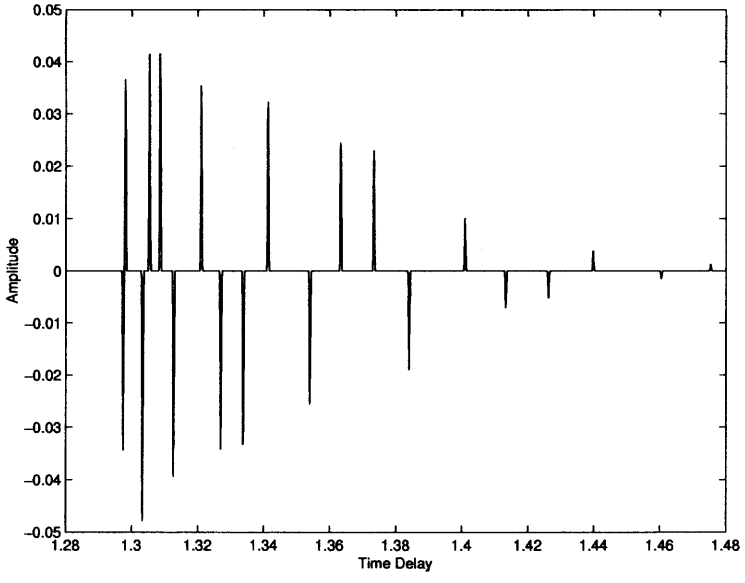

Figure 1.2 Signal obtained at the receiver.

The "spikes" in Figure 1.2 are the arrivals that we want to identify. Each arrival has a time delay, due to the varying arrival times of the multi-paths, and amplitude associated with it. The distinct arrivals correspond to rays which have travelled along different paths from the source to the receiver. The first arrival is typically the ray which travelled directly from the source to the receiver. The second arrival has often gone through one surface reflection before reaching the receiver. The surface reflected path is recognized by the change in polarity. The third arrival is the first

bottom bounce. The arrivals that follow are due to rays which have interacted with the surface, bottom, and bottom layers multiple times.

1.3 Replica Field Generation

Illustrative examples are presented here to show the effects the propagation environment has on the amplitudes and arrival times of a transmitted signal. In order to demonstrate these effects, synthetic fields need to be constructed. Sound propagation in the ocean is mathematically described by the wave equation. There are various models available (Normal modes, PE, ray theory, etc.) [6] which describe sound propagation in the ocean and can be used to calculate synthetic fields. Theoretical data is obtained by use of the Green's function, i.e., the solution of the wave equation describing propagation from a unit impulse source to an arbitrary location in the waveguide [6].

KRAKEN [7], a normal mode method, is used to obtain the received signals in Figure 1.3. Since the ultimate goal of this research is to simplify a highly complex problem, we illustrate this complexity by assuming that the source, receiver, and environmental parameters are known. The source is located 30 m below the ocean surface. The receiver is placed 50 m below the surface; its distance is 1 km away from the source. The depth of the water column is 115 m. The sound speed profile for the water decreases with depth, with a maximum speed of 1543 m/s near the surface of the ocean and a minimum speed of 1526 m/s near the bottom, typical of shallow water. We assume that the ocean bottom is composed of only one layer; below that layer will be a half-space (taken to be limestone). In each of the plots in Figure 1.3, the layer between the water and the half-space is different. Either the height of the sediment is changed (5 m, 20 m, or 50 m) or the sediment itself is changed (clay, sand, or chalk).

Table 1.1 gives the compressional sound speed for clay, sand, chalk and limestone [6] used to run KRAKEN.

Table 1.1 Sound Speeds for Ocean Bottoms Used in Figure 1.3

Sediment	Sound speed
Clay	1500 m/s
Sand	1650 m/s
Chalk	2400 m/s
Limestone	3000 m/s

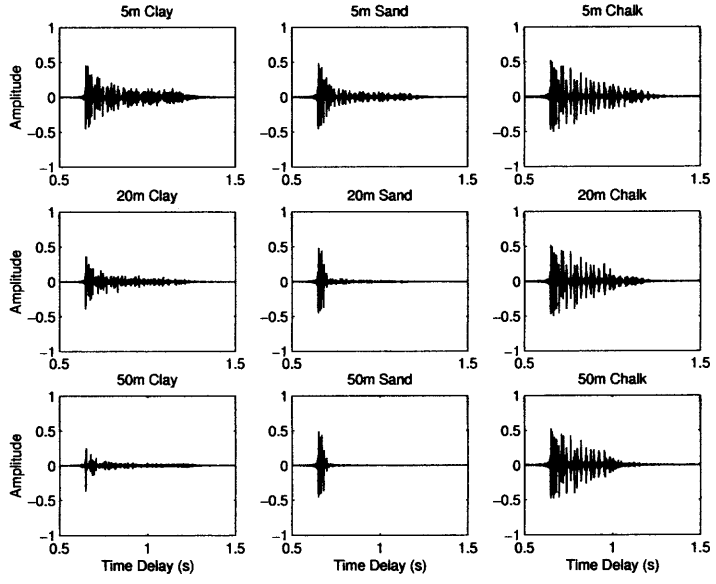

Figure 1.3 Signal obtained at the receiver with various bottom properties.

In a shallow water ocean environment, the sound speed in the ocean bottom, as well as the height of the sediment, significantly changes the appearance of the signal obtained at the receiver. As we move from left to right in Figure 1.3, the sound speed of the bottom sediment increases. We can see that increase in sound speed has

affected the amplitude of the signal, particularly at later times. As we move from top to bottom in Figure 1.3, the height of the bottom layer is increased while the sediment remains unchanged. Once again, we can see that a change in the height of the sediment has an impact on the signal. We have acquired simulated data for several test ocean bottom (basalt, limestone, chalk, moraine, gravel, sand, silt and clay for example) and various sediment heights. Studying the received signals, it is evident that the appearance of the signal is a direct consequence of the environment the signal propagated through.

A typical approach for extracting information from received acoustic fields is to use an inverse method which is generally cast as an optimization problem. In this framework, we will concentrate on the appearance of the received signal. The features associated with the signal we are interested in are the time delays and amplitudes of each arrival as well as the Signal to Noise Ratio (SNR). (Time delay and amplitude estimation is important in applications where a transmitted signal arrives at a receiving sensor through different propagation paths.) These features will form a basis for future estimation, reducing the computational time needed for the implementation of full-field inverse method. As shown in Figure 1.3, the various bottom sediments affect the amplitudes and the changes in sediment thickness affect the time delays. Therefore, the focus of this work is to develop an efficient method to easily recover these amplitudes and time delays, since they can provide significant information on the propagation environment and geometry.

This dissertation is structured as follows: In Chapter 2 a brief overview of methods typically applied to the problem at hand is provided. The Gibbs sampling algorithm is derived and results for amplitude and time delay estimation are presented and compared to other methods in Chapters 3 and 4. Noise is added in the estimation process in Chapter 5 and results are presented. In Chapter 6 the number of arrivals in the received signal is treated as an unknown. Chapter 7 deals with the issue of

convergence of the Gibbs sampling process. The number of arrivals, time delays, amplitudes, and noise level are estimated for the real data from the Haro Straight experiment in Chapter 8. Conclusions are given in Chapter 9.

CHAPTER 2

APPROACHES TO PARAMETER ESTIMATION PROBLEMS

Matched field processing (MFP) has been a popular approach for source localization and parameter estimation in the ocean [8, 9]. MFP is a full-field matching approach. It requires the replica field, which corresponds to theoretical array data, to be constructed for each test ocean environment. Maximization of similarity between the replicas, derived from the wave equation, and the data, measured at an array of sensors, is then employed using correlation techniques to determine parameter estimates. This process can become extremely computationally intensive due to the large number of parameters involved. For example, one may only be interested in locating the source, yet many other parameters associated with the environment such as sound speed profile, water depth, bottom properties, etc. need to be taken into account. Therefore, several approaches for reducing the computational requirements of MFP have been proposed [10, 11, 12, 5].

An alternative approach to MFP is to perform the estimation in two steps. The first step in the process is to obtain estimates for the parameters associated with the received signal, for example, the amplitudes and time delays, noise variance, the number of arrivals, etc. These estimates can then be used to quickly find estimates for the parameters associated with the problem of interest, such as source and receiver location, sound speed profile, bottom properties, etc. This work will focus on the first step; we will concentrate only on select features of the synthetic field, extending work presented in [12, 13, 14, 5, 15].

Previous work has been done on amplitude and arrival time estimation. Analytical Estimation [16], Matched Filter (MF) [16, 17], Expectation Maximization (EM) [12, 18], and Simulated Annealing (SA) algorithms [13] have been implemented to

identify these features. In this work, we develop a Gibbs sampling approach for amplitude and arrival time estimation. We will compare our results using Gibbs sampling to those obtained using the analytical estimation method, MF, EM, and SA. Therefore, for the sake of completeness, we will provide a brief outline of the major components involved in analytical estimation [16], MF [16, 17], EM [12], and SA [10, 11, 13, 19].

In this paper, the method referred to as the analytical method is a maximum-likelihood procedure for estimating the amplitudes and arrival times of individual pulses in the multi-path signal [16]. Estimates of the N sets of amplitude and arrival times can be obtained by formulating a 2N parameter estimation problem. First, the maximum-likelihood estimates of arrival times for N pulses are obtained by finding the maximum over n_i of $\Phi^T \Lambda \Phi$ where Φ is the vector of matched filter outputs for a particular set of arrival times n_i and Λ is the cross-correlation matrix for the N signals with delays $n_1, n_2, ..., n_N$. In general, there is no simple technique for finding this maximum. The only recourse is to calculate $\Phi^T \Lambda \Phi$ over a N-dimensional volume in time space. The resulting set of arrival time estimates is then used in $A = \Lambda^{-1}\Phi$ to obtain the amplitude estimates. The computational demands required by this estimation method quickly becomes overwhelming when the signal at hand has four arrivals or more.

A Matched Filter (MF) can be used to recover the amplitudes and time delays of a received signal. MF is favorable due to the ease in which it is implemented, simply correlating each arrival in the received signal with the transmitted waveform [16, 17]. The time at which the filter output peaks gives the arrival time and the height of the peak gives the amplitude. Difficulty will arise with the MF technique when the arrival times of the received signal are close. Resolving individual waveforms in the case of overlapping arrivals using MF could be erroneous [2, 13]. However, it can be shown that, if the arrivals are separated in time by more than the duration of the

signal autocorrelation function, MF is equivalent to maximum likelihood estimation (MLE) [16].

The EM algorithm is an iterative technique for solving MLE problems [12, 20]. The algorithm starts with an initial guess. EM is a two step process involving the log-likelihood of the observed data. The first step is to compute the conditional expected value of the unknown parameters given a signal. The second step in the EM algorithm is to maximize the expected value found in the first step over all the unknown parameters. EM is fast and works well with the proper initial conditions. However, its performance is highly dependent on the initial conditions; the method is quick to converge to a local maximum. As in all "hill climbing" techniques there is no guarantee of convergence to a global maximum. Therefore, a "randomized hill climbing" technique, referred to as SA, is more promising from this aspect, although for this scheme global convergence in practice is not guaranteed [12, 21, 22] either.

SA is a Monte Carlo optimization approach [23]; it arose from the technique used to slowly cool liquid metal to a crystal of minimum energy. Each parameter is given an initial value. This initial value is perturbed through an addition of a random component. The algorithm begins at a "high" temperature T. This temperature, when high, increases the probability that we will accept the new values for the parameters regardless of whether they are good or not. As the temperature decreases, so does the probability of accepting a "bad" value. Starting at a "high" temperature allows the algorithm to jump out of local minima. The core of SA is choosing the appropriate cost function, annealing schedule, and suitable parameter perturbations. The cost function is the quantity we wish to minimize (like the energy of the crystal). The annealing schedule determines how T will be decreased. Choosing the appropriate cost function and a good cooling schedule is critical to the success of an SA algorithm.

In this work, we present a novel method for estimation of time delays, amplitudes, and number of multi-paths, as well as noise variance with a maximum a posteriori

estimation approach. Maximum a posteriori estimation is optimal if the appropriate statistical models are selected for the received data. We propose a method of maximum a posteriori estimation in which optimization is performed using Gibbs sampling [24, 25, 26, 27, 28].

CHAPTER 3

GIBBS SAMPLING FOR PARAMETER ESTIMATION

To efficiently estimate the arrival times and amplitudes of a multi-path signal, we propose a scheme that maximizes the posterior probability density function of those unknowns. Noise variance and number of arrivals of arrivals are presently considered as known parameters; this assumption will be removed in future chapters. To obtain the posterior distribution of the arrival times and amplitudes, a standard Bayesian approach is followed. That is, given received data, r, and a set of unknown parameters, α, the joint probability distribution, $p(r, \alpha)$, is

$$p(r, \alpha) = p(r|\alpha)p(\alpha) = p(\alpha|r)p(r), \tag{3.1}$$

and the a posteriori probability of α is given by:

$$p(\alpha|r) = \frac{p(r|\alpha)p(\alpha)}{p(r)}. \tag{3.2}$$

Selecting the values of α that maximize $p(\alpha|r)$ is known as maximum a posteriori (MAP) estimation [29, 26]. Since $p(r)$ is independent of the parameter α, maximizing the a posteriori density is equivalent to maximizing the product $p(r|\alpha)p(\alpha)$ [29]. The method is very powerful. The results, however, are dependent on the accuracy of the statistical model $p(r|\alpha)$ and the nature of prior beliefs encapsulated in $p(\alpha)$.

In [29] it is shown that if the prior distribution of α is broad and void of peaks, there is a lack of any real knowledge on parameter α, except potentially for the limits on the range of α. In this event, maximizing $p(\alpha|r)$ is equivalent to maximizing $p(r|\alpha)$, which is known as maximum-likelihood estimation. As shown in [16], this is the optimal approach to estimating time delays between distinct signals and their corresponding amplitudes in a white Gaussian noise environment (a simple matched

filter is not optimal for overlapping arrivals). This maximization given observed data leads to an analytical expression for the amplitudes, whereas time delays can be obtained by identifying where the maximum of an M dimensional function occurs, where M is the known number of paths [16]. When M is large, time delay estimation becomes a computationally cumbersome task.

To alleviate some of the computational demands, we will use a Gibbs sampling technique to efficiently estimate the posterior distribution of all unknown parameters [24, 25]. The Gibbs sampler is a Monte Carlo Markov Chain approach for the calculation of a numerical estimate of posterior probability distributions. In [26, 27, 25, 28] it is shown that the posterior distribution to be estimated is uniquely determined through the conditional distributions of individual parameters.

3.1 Derivation of the Gibbs Sampler

In order to implement the Gibbs sampler for the purpose of estimating the unknown parameters in our problem, the conditional distributions of time delays and amplitudes need to be obtained. Equation 1.1 is used as a model for the received signal, where $w(n)$ is white Gaussian noise with zero mean and noise variance σ^2.

In our case, the amplitudes are real numbers and the sign indicates their polarity. Since this is the only prior information available on the amplitudes, uniform, non-informative prior distributions for these parameters are assumed. That is,

$$p(a_i) = 1, \quad -\infty < a_i < +\infty, \quad i = 1, ..., M. \tag{3.3}$$

For the time delays, we will assume uniform priors for arrival times that vary between 1 and N, i.e.,

$$p(n_i) = \frac{1}{N}, \quad 1 \leq n_i \leq N, \quad i = 1, ..., M. \tag{3.4}$$

The joint posterior probability distribution function of all unknown parameters a_i and n_i, $i = 1, ..., M$ given observed data $r(n)$ can be written as follows [30, 31, 32]:

$$p(n_1, ..., n_M, a_1, ..., a_M | r(n)) =$$
$$K \frac{1}{N^M} \frac{1}{(\sqrt{2\pi})^N \sigma^N} exp(-\frac{1}{2\sigma^2} \sum_{n=1}^{N} (r(n) - \sum_{i=1}^{M} a_i s(n - n_i))^2), \tag{3.5}$$

where $1/K$ is the N-dimensional joint probability density function of $r(n)$, $n = 1, ..., N$, which is a constant. Equation 3.5 can be simplified by consolidating all constants:

$$p(n_1, ..., n_M, a_1, ..., a_M | r(n)) =$$
$$Cexp(-\frac{1}{2\sigma^2} \sum_{n=1}^{N} (r(n) - \sum_{i=1}^{M} a_i s(n - n_i))^2). \tag{3.6}$$

From this joint posterior probability distribution function, an expression for the conditional distribution of a_i can be obtained assuming all a_j, $j = 1, ..., M$, $j \neq i$ and all n_k, $k = 1, ..., M$ are known. From Equation 3.6, the marginal posterior distribution for a_i can be obtained:

$$p(a_i | n_1, ..., n_M, a_1, ..., a_{i-1}, a_{i+1}, ..., a_M, r(n)) =$$
$$Dexp(-\frac{1}{2\sigma^2}(a_i - (\sum_{n=1}^{N} r(n)s(n - n_i) - \sum_{j=1(j\neq i)}^{M} a_j \sum_{n=1}^{N} s(n - n_i)s(n - n_j)))^2), \tag{3.7}$$

where D is the normalization constant of the distribution. The distribution of Equation 3.7 can be identified to be Gaussian with mean

$$\sum_{n=1}^{N} r(n)s(n - n_i) - \sum_{j=1(j\neq i)}^{M} a_j \sum_{n=1}^{N} s(n - n_i)s(n - n_j) \tag{3.8}$$

and variance σ^2.

The conditional posterior distributions for time delays n_i, $i = 1, ..., M$ are obtained on a grid. Assuming a_j, $j = 1, ..., M$ and n_k, $k = 1, ..., M$, $k \neq i$ are known, the conditional distribution of n_i is written:

$$p(n_i|n_1, ..., n_{i-1}, n_{i+1}, ..., n_M, a_1, ..., a_M, r(n)) = Gexp(-\frac{1}{2\sigma^2}\sum_{n=1}^{N}(r(n) - \sum_{i=1}^{M} a_i s(n - n_i))^2) \tag{3.9}$$

where G is the normalization constant of the distribution.

3.2 Gibbs Sampling Implementation

Gibbs sampling is a Monte Carlo Markov Chain approach that can be used to obtain estimates for the arrival times and amplitudes of the distinct arrivals. It is a technique for generating random samples from a joint posterior distribution indirectly by drawing samples from conditional distributions [24, 28]. The Gibbs sampling Markovian updating scheme proceeds as follows.

Given a received signal with M distinct arrivals, the algorithm begins by assigning initial values to the $2M$ unknown parameters (each arrival has a time delay and an amplitude associated with it). The Gaussian distribution of Equation 3.7 is used to generate a sample for a_1, which is conditional on all $2M - 1$ other parameters involved in the estimation. Using this new value for a_1, a sample is generated for a_2. The updating process continues until a sample is generated for all a_i, $i = 1, ..., M$. The conditional distribution, Equation 3.9, is then used to obtain samples for each n_i. However, since the posterior distributions of the time delays are not analytically tractable, the distribution in Equation 3.9 will be calculated on a grid. Once a sample has been generated for all $2M$ parameters one iteration is complete and the process is continued repeatedly until many samples have been drawn for all parameters. Reference [26] shows that under mild conditions, after many iterations, the samples generated can be regarded as simulated observations from the true joint distribution.

And so, Gibbs sampling is based only on elementary properties of Markov chains and avoids difficult calculations, replacing them instead with a sequence of easier calculations [28].

Investigations have shown that iterative sampling achieved through Gibbs samplers is efficient, converging quickly for a wide range of problems. Advocacy of the approach rests on its simplicity and universality but not on any claim that it is the most efficient procedure for any given problem [27]. This work will show that, for the purpose of estimating time delays and amplitudes, the algorithm is not only accurate and efficient but is also more informative than other estimation methods. It provides estimates of the posterior probability distribution functions in addition to point estimates typically provided by other approaches.

CHAPTER 4

PERFORMANCE EVALUATION OF ESTIMATION APPROACHES

In this chapter the proposed Gibbs sampling algorithm is tested on synthetic data and compared to the optimal analytical method [16], MF, EM, and SA. Numerous received signals are numerically simulated. These five methods are then used to calculate estimates for the time delays and amplitudes for each arrival. Error measures are then calculated in order to compare the performance of each algorithm. Also presented in this chapter is an example in which one run of the Gibbs sampler appears to fail to locate all the arrivals present in the received signal when only looking at the point estimates obtained. However, it is shown that the distribution of all samples generated provides information on the missed arrival.

4.1 Signal Generation

Received signals are numerically generated for two source signals. The first source sequence is the broad in time, truncated sinc pulse shown in Figure 4.1. The second source used to generate replicas of transmitted signals is the more narrow sinc pulse shown in Figure 4.2. Arranging these signals at different places in time with various amplitudes creates signals similar to those generated when a pulse travels to a receiver by way of many paths.

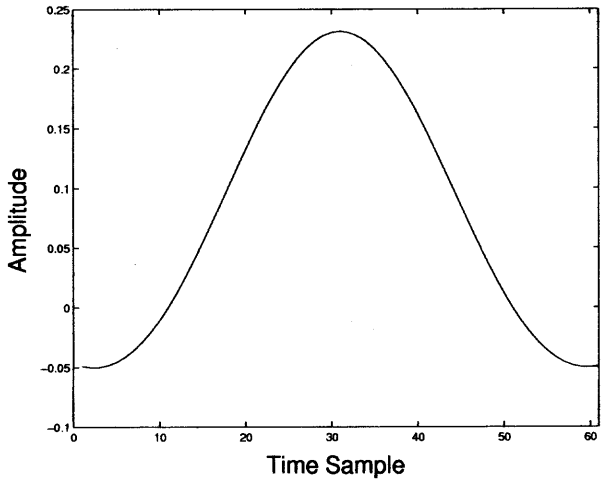

Figure 4.1 Broad in time source signal.

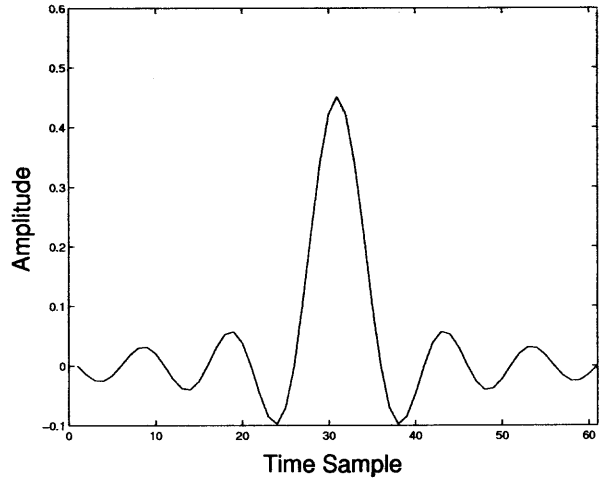

Figure 4.2 Narrow in time source signal.

Given a transmitted signal, we will consider cases in which two and three arrivals are present in the received signal. Figure 4.3 is an example of a received signal without noise for two very closely spaced arrivals using the broad source pulse in Figure 4.1. Figure 4.4 is an example of a received signal without noise for three widely spaced arrivals using the narrow source pulse in 4.2.

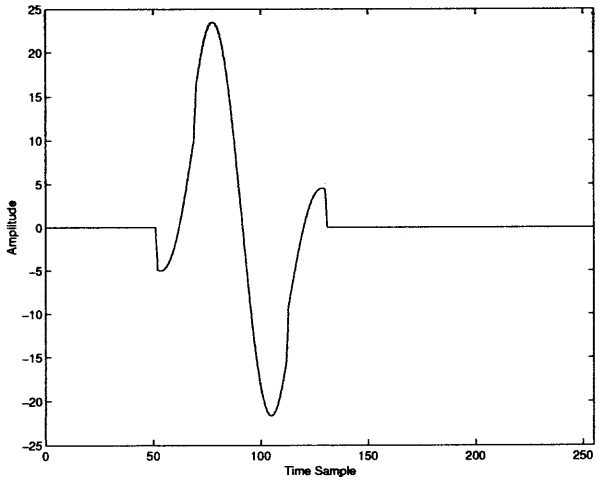

Figure 4.3 Signal consisting of two arrivals closely spaced without noise for the broad transmitted signal.

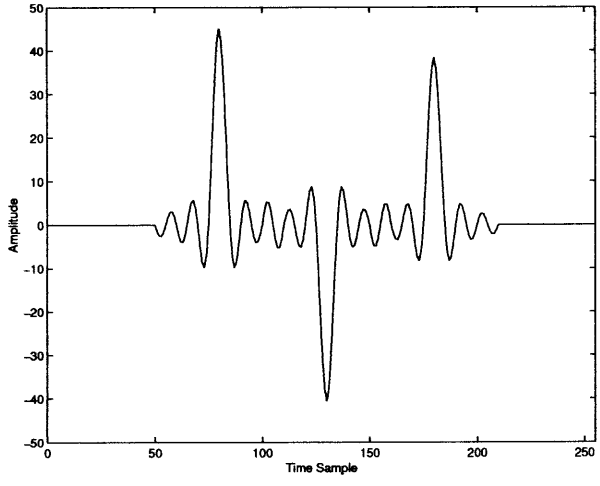

Figure 4.4 Signal consisting of three arrivals widely spaced without noise for the narrow transmitted signal.

The final step in the signal generation is to include the effects of noise in the transmitted signal. Random noise with variance ranging from 0.01 to 0.1 is then added to the multi-path signals to simulate realistic receptions. Noisy signal realizations are presented in Figures 4.5 through 4.7.

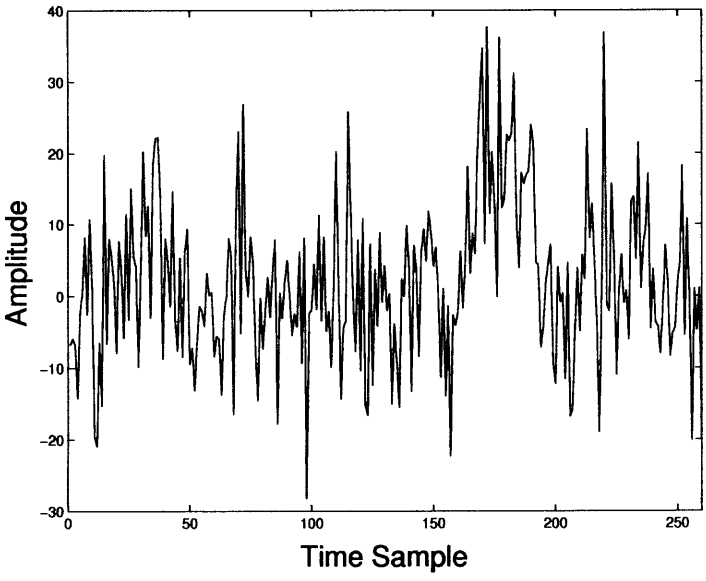

Figure 4.5 Signal obtained at the receiver for three arrivals with noise variance 0.01.

Signals are generated by varying the number of arrivals, the time delay and amplitude associated with each arrival, and the noise variance. For each case, 100 realizations are generated from which the amplitudes and delays are estimated by all five algorithms.

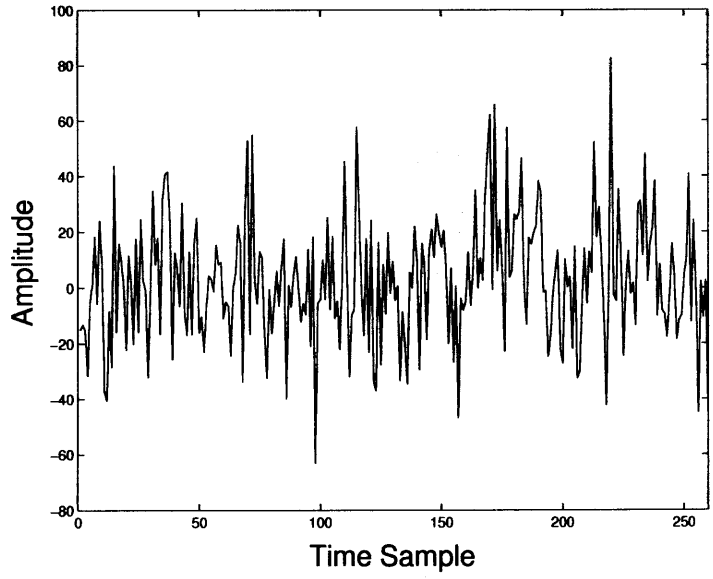

Figure 4.6 Signal obtained at the receiver for three arrivals with noise variance 0.05.

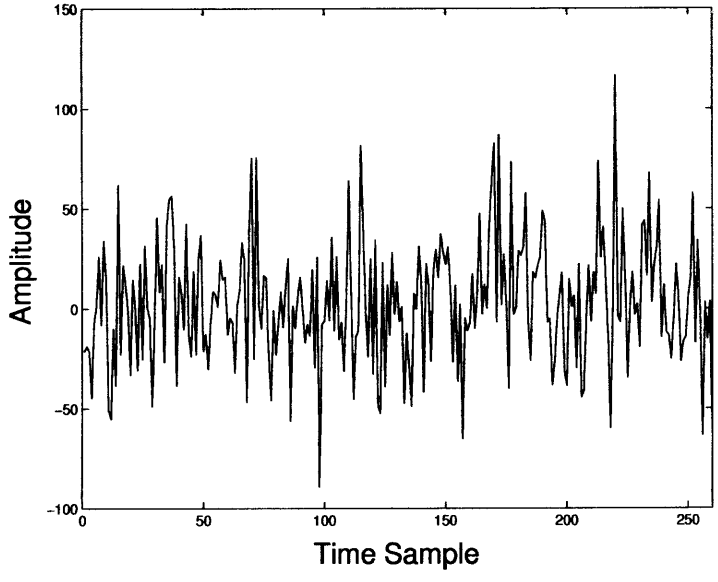

Figure 4.7 Signal obtained at the receiver for three arrivals with noise variance 0.1.

4.2 Error Analysis

To quantify the results generated by the five comparative methods, the following error analysis is adopted. First, the combined errors L_1 and L_2 [33], based on the estimates obtained for all unknown parameters, are calculated from the following equations. According to [33], estimations are considered excellent when $L_1 \leq 0.1$.

$$L_1 = \frac{1}{M(I_{max} - I_{min})} \sum_{i=1}^{M} |\hat{x}_i - x_i| \tag{4.1}$$

$$L_2 = \frac{1}{\sqrt{M}} \left[\sum_{i=1}^{M} \left(\frac{\hat{x}_i - x_i}{I_{max} - I_{min}} \right)^2 \right]^{\frac{1}{2}} \tag{4.2}$$

where, $i = 1, ..., M$ is the number of unknown parameters,

$\hat{x}_i$ is the estimate value for the ith parameter,

x_i is the true value for the ith parameter, and

(I_{min}, I_{max}) is the search interval for the ith parameter.

Additional information about the accuracy of the estimates for the distinct arrivals is obtained by calculating an error for each individual parameter using the following equation.

$$P_i = \left| \frac{\hat{x}_i - x_i}{I_{max} - I_{min}} \right|^2 \tag{4.3}$$

where, $i = 1, ..., M$ is the number of unknown parameters,

$\hat{x}_i$ is the estimate value for the ith parameter,

x_i is the true value for the ith parameter,

I is the $\max(x_i - I_{min},\ I_{max} - x_i)$ and (I_{min}, I_{max}) is the search interval for the ith parameter.

One hundred signals were generated from which the amplitudes and delays were estimated by all five algorithms. Presented in the tables that follow are the mean

errors from these 100 runs. The first set of results correspond to the broad transmitted signal in Figure 4.1. Two arrivals are present; the true delays and amplitudes are given in Table 4.1. The amount of added noise varies. Tables 4.2 through 4.4 display the mean errors for signals generated with noise variance 0.01; Tables 4.5 through 4.7 are the mean errors for signals with noise variance 0.05; and Tables 4.8 through 4.10 display the mean errors for signals with noise variance 0.1.

Table 4.1 True Time Delays and Amplitudes for Two Arrivals

Arrival	Time delay	Amplitude
1	50	100
2	52	-90

Table 4.2 Mean L_1 and L_2 Errors for Two Arrivals With Noise Variance 0.01

Method	Mean L_1 Error	Mean L_2 Error
Analytical	0.0054	0.0075
Gibbs Sampling	0.0054	0.0075
MF	0.0595	0.1061
EM	0.0612	0.1090
SA	0.0472	0.1017

Table 4.3 Mean Time Delay Errors Using P_i for Two Arrivals With Noise Variance 0.01

Method	Delay 1	Delay 2	Average
Analytical	0.00001	0.00003	0.00002
Gibbs Sampling	0.00001	0.00003	0.00002
MF	0.0040	0.0065	0.0053
EM	0.0084	0.0072	0.0078
SA	0.0040	0.0276	0.0158

Table 4.4 Mean Amplitude Errors Using P_i for Two Arrivals With Noise Variance 0.01

Method	Delay 1	Delay 2	Average
Analytical	0.0002	0.0002	0.0002
Gibbs Sampling	0.0002	0.0002	0.0002
MF	0.0028	0.0030	0.0029
EM	0.0031	0.0035	0.0033
SA	0.0022	0.0023	0.0023

The Gibbs sampling results, Tables 4.2 through 4.4, for this case are practically identical to the optimal analytical results. Although all five methods satisfy the condition stated in [33], $L_1 \leq 0.1$, and, hence, all results are considered excellent, the superiority of Gibbs sampling is clearly evident. MF has difficulty resolving closely spaced arrivals. Regardless of the initial conditions chosen for this case, and many different combinations were tried, the EM estimates differ in general from the true values. The results presented in this paper, unless otherwise stated, all methods

requiring initial conditions, Gibbs sampling, EM, and SA, are started with the same initial conditions for fair comparison. SA was generally unable to recover the second arrival.

Table 4.5 Mean L_1 and L_2 Errors for Two Arrivals With Noise Variance 0.05

Method	Mean L_1 Error	Mean L_2 Error
Analytical	0.0447	0.0908
Gibbs Sampling	0.0447	0.0917
MF	0.0787	0.1714
EM	0.0878	0.2001
SA	0.1061	0.2827

Table 4.6 Mean Time Delay Errors Using P_i for Two Arrivals With Noise Variance 0.05

Method	Delay 1	Delay 2	Average
Analytical	0.0029	0.0242	0.0136
Gibbs Sampling	0.0029	0.0249	0.0138
MF	0.0087	0.0502	0.0295
EM	0.0145	0.0491	0.0318
SA	0.0115	0.1252	0.0684

Table 4.7 Mean Amplitude Errors Using P_i for Two Arrivals With Noise Variance 0.05

Method	Delay 1	Delay 2	Average
Analytical	0.0030	0.0031	0.0031
Gibbs Sampling	0.0030	0.0031	0.0031
MF	0.0029	0.0038	0.0034
EM	0.0034	0.0038	0.0036
SA	0.0036	0.0037	0.0037

The Gibbs sampling results, Tables 4.5 through 4.7, for this case are nearly identical to the optimal analytical results. Since this signal is the same as in the previous example (only with more added noise), it was expected that MF would not perform very well. The performance of the EM approach has not changed from the previous case. Once again the SA method was unable to recover the second arrival.

Table 4.8 Mean L_1 and L_2 Errors for Two Arrivals With Noise Variance 0.1

Method	Mean L_1 Error	Mean L_2 Error
Analytical	0.0880	0.1903
Gibbs Sampling	0.0925	0.2040
MF	0.1014	0.2358
EM	0.1042	0.2567
SA	0.1254	0.3337

Table 4.9 Mean Time Delay Errors Using P_i for Two Arrivals With Noise Variance 0.1

Method	Delay 1	Delay 2	Average
Analytical	0.0204	0.0642	0.0425
Gibbs Sampling	0.0215	0.0787	0.0501
MF	0.0335	0.0839	0.0587
EM	0.0166	0.0876	0.0521
SA	0.0252	0.1456	0.0854

Table 4.10 Mean Amplitude Errors, P_i, for Two Arrivals With Noise Variance 0.1

Method	Delay 1	Delay 2	Average
Analytical	0.0075	0.0075	0.0075
Gibbs Sampling	0.0070	0.0069	0.0069
MF	0.0031	0.0039	0.0035
EM	0.0034	0.0038	0.0036
SA	0.0037	0.0036	0.0036

According to [33] the analytical method and Gibbs sampling results are considered excellent estimates, Tables 4.8 through 4.10; whereas MF, EM, and SA perform poorly for this last case. Although the additional information provided by the amplitude error analysis is beneficial, it is only useful if the delay is correctly located in time. Otherwise the occurrence of an incorrectly estimated delay is actually a fabrication of the noise present in the signal and the associated amplitude is not the amplitude of an arrival but rather noise. Thus, the error analysis for the amplitude estimates could be somewhat misleading.

To further compare performance the five algorithms, in particular relative to arrival times, the mean L_1 and L_2 errors for the delays alone were computed and are now presented in Figures 4.8 through 4.10 and in Tables 4.11 to 4.13. Two arrivals are considered in which the separation between the arrivals varies from 2 to 20.

Figures 4.8, 4.9 and 4.10 plot the mean L_1 errors for the time delays only for the given signals with noise variance 0.01, 0.05 and 0.1 respectively. Each line graphs the mean error from one hundred runs of the various estimation methods. In each run the signal and initial guesses remain the same, the noise varies. The blue lines trace the error for the analytical results, red is used for Gibbs sampling, MF errors are plotted in green, EM in black, and SA in yellow. It is clear that Gibbs sampling is the method most comparable to the analytical method. It is also easy to see in these results that the performance of MF improves as the time between the arrivals increases. EM results, compared to the analytical and Gibbs sampling results, are mostly disappointing. This issue will be addressed later in this chapter. Overall, the results for SA are poor.

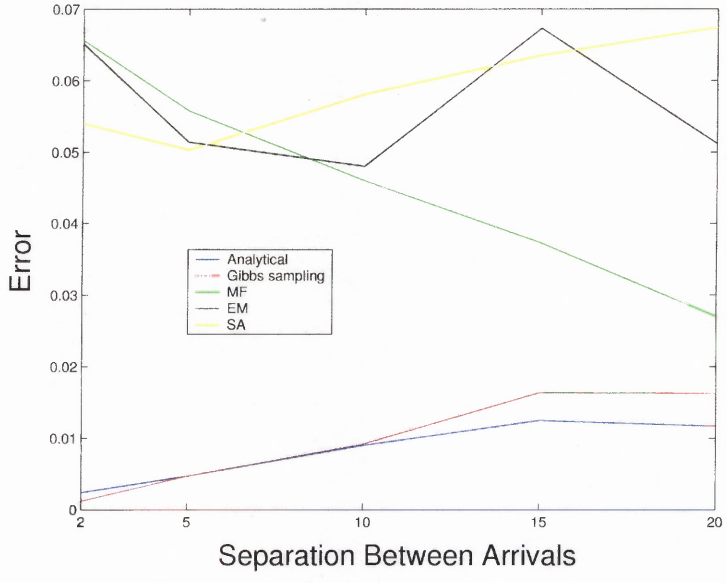

Figure 4.8 Mean L_1 errors for delays only with noise variance 0.01.

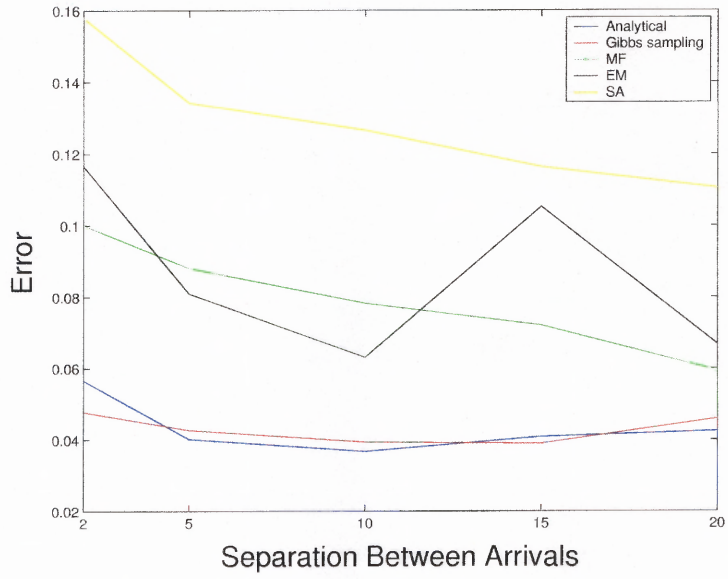

Figure 4.9 Mean L_1 errors for delays only with noise variance 0.05.

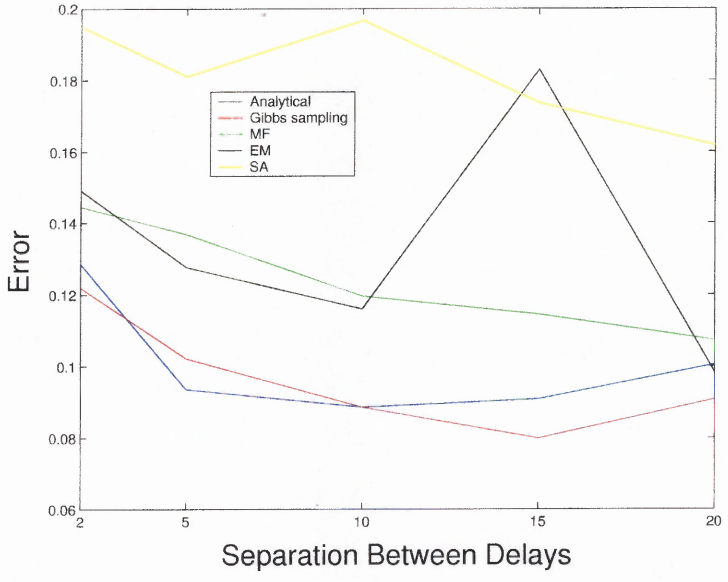

Figure 4.10 Mean L_1 errors for delays only with noise variance 0.1.

Tables 4.11, 4.12, and 4.13 present the L_2 errors for the time delays only for the given signals with noise variance 0.01, 0.05, and 0.1 respectively. Each column gives the mean error from one hundred runs of the given estimation method. The first column contains the mean errors for received signals which have delays separated by 2 units of time. In column 2 the delays are 5 units apart, followed by delays 10 units apart. Columns 4 and 5 are the mean errors for signals separated by 15 and 20 units of time, respectively. Again, it is clear that Gibbs sampling is the method most comparable to the analytical method. It is also clear in these results that the performance of MF improves as the time between the arrivals increases. EM results, compared to the analytical and Gibbs sampling results, are good on some occasions however not for all cases. Overall, the results for SA are poor.

Table 4.11 Mean L_2 Errors for Delays Only With Noise Variance 0.01

Method	Delays 50 and 52	Delays 50 and 55	Delays 50 and 60	Delays 50 and 65	Delays 50 and 70
Analytical	0.00004	0.00009	0.0002	0.0003	0.0003
Gibbs Sampling	0.00002	0.00009	0.0002	0.0004	0.0009
MF	0.0053	0.0033	0.0023	0.0018	0.0013
EM	0.0078	0.0028	0.0028	0.0064	0.0049
SA	0.0158	0.0104	0.0117	0.0152	0.0154

Table 4.12 Mean L_2 Errors for Delays Only With Noise Variance 0.05

Method	Delays 50 and 52	Delays 50 and 55	Delays 50 and 60	Delays 50 and 65	Delays 50 and 70
Analytical	0.0193	0.0098	0.0053	0.0054	0.0040
Gibbs Sampling	0.0138	0.0117	0.0067	0.0052	0.0060
MF	0.0295	0.0186	0.0156	0.0142	0.0102
EM	0.0318	0.0162	0.0062	0.0207	0.0094
SA	0.0684	0.0525	0.0492	0.0397	0.0347

Table 4.13 Mean L_2 Errors for Delays Only With Noise Variance 0.1

Method	Delays 50 and 52	Delays 50 and 55	Delays 50 and 60	Delays 50 and 65	Delays 50 and 70
Analytical	0.0544	0.0326	0.0264	0.0256	0.0304
Gibbs Sampling	0.0502	0.0391	0.0263	0.0190	0.0237
MF	0.0589	0.0564	0.0375	0.0350	0.0321
EM	0.0522	0.0420	0.0353	0.0692	0.0251
SA	0.0856	0.0711	0.0827	0.0728	0.0568

The next set of results are for the broad transmitted signal in Figure 4.1. Three arrivals are present; the delays and amplitudes for these arrivals are given in Table 4.14. Tables 4.15 through 4.17 display the mean errors for signals generated with noise variance 0.01. Once again, it is shown that the Gibbs sampling algorithm is a good match to the analytical method. The separation between the first and second arrival is narrow relative to the width of the transmitted signal and hence MF has difficulty locating the second delay. In this case, SA outperforms EM, however neither method fairs well compared to the other three in this case.

Table 4.14 True Time Delays and Amplitudes Spaced Signals

Arrival	Time delay	Amplitude
1	10	100
2	15	-90
3	150	85

Table 4.15 Mean L_1 and L_2 Errors for Signal Described in Table 4.14

Method	Mean L_1 Error	Mean L_2 Error
Analytical	0.0331	0.1049
Gibbs Sampling	0.0317	0.0870
MF	0.0731	0.2632
EM	0.2449	0.9402
SA	0.1082	0.4057

Table 4.16 Mean Time Delay Errors Using P_i for Signal Described in Table 4.14

Method	Delay 1	Delay 2	Delay 3	Average
Analytical	0.0015	0.0371	0.0017	0.0135
Gibbs Sampling	0.0020	0.0220	0.0001	0.0083
MF	0.0134	0.1289	0.0024	0.0482
EM	0.4502	0.4602	0.00005	0.3035
SA	0.0261	0.1815	0.0375	0.0817

Table 4.17 Mean Amplitude Errors Using P_i for Signal Described in Table 4.14

Method	Delay 1	Delay 2	Delay 3	Average
Analytical	0.0013	0.0017	0.0004	0.0011
Gibbs Sampling	0.0039	0.0039	0.0001	0.0026
MF	0.0026	0.0046	0.0003	0.0025
EM	0.0029	0.0051	0.0014	0.0032
SA	0.0044	0.0066	0.0018	0.0043

Next, once again three arrivals are considered. The first and second arrivals are now further apart than in the previous example (Table 4.18). Results for the same noise variance are presented in Tables 4.19 through 4.21. The Gibbs sampler is a close second to the performance of the analytical method. Although the MF errors here are lower for this signal than it was in the previous example, the separation between the delays are still too narrow relative to the width of the transmitted signal for it to perform as well as the analytical method. The initial conditions chosen this time enhanced the performance of EM.

Table 4.18 True Time Delays and Amplitudes

Arrival	Time delay	Amplitude
1	10	100
2	30	-90
3	150	85

Table 4.19 Mean L_1 and L_2 Errors for Signal Described in Table 4.18

Method	Mean L_1 Error	Mean L_2 Error
Analytical	0.0115	0.0252
Gibbs Sampling	0.0187	0.0360
MF	0.0592	0.2281
EM	0.0354	0.1207
SA	0.0736	0.2622

The set of results that follow are for the narrow in time transmitted signal of Figure 4.2. Three arrivals are present; the delays and amplitudes for the these arrivals are given in Table 4.22. The separation between the first and second delays is further increased. Tables 4.23 through 4.25 display the mean errors for signals generated. In this case, MF compares well to the analytical method and Gibbs sampling because of the characteristics of the received signal.

Table 4.20 Mean Time Delay Errors Using P_i for Signal Described in Table 4.18

Method	Delay 1	Delay 2	Delay 3	Average
Analytical	0.00003	0.00002	0.00001	0.00002
Gibbs Sampling	0.00005	0.00004	0.00001	0.00003
MF	0.0067	0.0524	0.0598	0.0397
EM	0.0019	0.0317	0.0207	0.0181
SA	0.0064	0.0671	0.0606	0.0447

Table 4.21 Mean Amplitude Errors Using P_i for Signal Described in Table 4.18

Method	Delay 1	Delay 2	Delay 3	Average
Analytical	0.0003	0.0005	0.00006	0.0003
Gibbs Sampling	0.0029	0.0032	0.00009	0.0020
MF	0.0016	0.0046	0.0023	0.0029
EM	0.0019	0.0021	0.0005	0.0015
SA	0.0029	0.0055	0.0033	0.0039

The following set of results are for the broad in time transmitted signal of Figure 4.1. Three arrivals are present; the delays and amplitudes for the these arrivals are given in Table 4.14. Tables 4.26 through 4.28 display the mean errors for signals generated with noise variance 0.05. Again, Gibbs sampling is second only to the analytic method with SA coming in third this case.

Table 4.22 True Time Delays and Amplitudes

Arrival	Time delay	Amplitude
1	50	100
2	100	-90
3	150	85

Table 4.23 Mean L_1 and L_2 Errors for Signal in Described Table 4.22

Method	Mean L_1 Error	Mean L_2 Error
Analytical	0.0067	0.0144
Gibbs Sampling	0.0068	0.0145
MF	0.0071	0.0148
EM	0.1326	0.4744
SA	0.0721	0.2140

The next set of results are for the narrow in time transmitted signal of Figure 4.2. Three arrivals are present; the delays and amplitudes for the these arrivals are given in Table 4.18. Tables 4.29 through 4.31 display the mean errors for signals generated with noise variance 0.05. EM does well here compared to the analytic method and Gibbs sampling because the chosen initial conditions were close to the true parameters' values.

Table 4.24 Mean Time Delay Errors Using P_i for Signal Described in Table 4.22

Method	Delay 1	Delay 2	Delay 3	Average
Analytical	0.0006	0.0011	0.0006	0.0008
Gibbs Sampling	0.0006	0.0011	0.0006	0.0008
MF	0.0006	0.0013	0.0006	0.0009
EM	0.0419	0.0478	0.1471	0.0789
SA	0.0108	0.0284	0.0174	0.0189

Table 4.25 Mean Amplitude Errors Using P_i for Signal Described in Table 4.18

Method	Delay 1	Delay 2	Delay 3	Average
Analytical	0.0001	0.0003	0.0002	0.0002
Gibbs Sampling	0.0001	0.0003	0.0002	0.0002
MF	0.0002	0.0004	0.0002	0.0003
EM	0.0026	0.0053	0.0028	0.0035
SA	0.0038	0.0076	0.0027	0.0047

The following set of results are for the narrow in time transmitted signal of Figure 4.2. Three arrivals are present; the delays and amplitudes for the these arrivals are given in Table 4.22. Tables 4.32 through 4.34 display the mean errors for signals generated with noise variance 0.05. Gibbs sampling, MF, and SA all provide results comparable to the analytic. However, once again we see EM's dependence on the initial conditions, which in this case were chosen far from the true values.

Table 4.26 Mean L_1 and L_2 Errors for Arrivals Described in Table 4.14

Method	Mean L_1 Error	Mean L_2 Error
Analytical	0.1189	0.4273
Gibbs Sampling	0.1365	0.4366
MF	0.1644	0.6250
EM	0.2178	0.8378
SA	0.1611	0.5672

Table 4.27 Mean Time Delay Errors Using P_i for Arrivals Described in Table 4.14

Method	Delay 1	Delay 2	Delay 3	Average
Analytical	0.0577	0.2144	0.0095	0.0939
Gibbs Sampling	0.0846	0.2021	0.0089	0.0985
MF	0.1523	0.3263	0.0124	0.1637
EM	0.3261	0.4197	0.0075	0.2511
SA	0.1029	0.2673	0.0325	0.1342

The set of results that follow are for the broad in time transmitted signal of Figure 4.1. Three arrivals are present; the delays and amplitudes for the these arrivals are given in Table 4.18. Tables 4.35 through 4.37 display the mean errors for signals generated with noise variance 0.1. In this case, looking only at the L_1 and L_2 errors it appears that Gibbs sampling fails. However the errors for the individual parameters shows that it does find the time delays in accordance with the analytic method and the excessive error is due to the amplitude estimation in this case.

Table 4.28 Mean Amplitude Errors Using P_i for Arrivals Described in Table 4.14

Method	Delay 1	Delay 2	Delay 3	Average
Analytical	0.0045	0.0075	0.0022	0.0047
Gibbs Sampling	0.0187	0.0244	0.0043	0.0158
MF	0.0032	0.0096	0.0010	0.0046
EM	0.0035	0.0055	0.0013	0.0034
SA	0.0053	0.0096	0.0033	0.0061

Table 4.29 Mean L_1 and L_2 Errors for Arrivals Described in Table 4.18

Method	Mean L_1 Error	Mean L_2 Error
Analytical	0.0684	0.2529
Gibbs Sampling	0.0778	0.2801
MF	0.0831	0.3032
EM	0.0791	0.3031
SA	0.1098	0.3854

The final set of results are for the narrow in time transmitted signal of Figure 4.2. Three arrivals are present; the delays and amplitudes for the these arrivals are given in Table 4.22. Tables 4.38 through 4.40 display the mean errors for signals generated with noise variance 0.1. Once again, the reliability of Gibbs sampling is confirmed.

Table 4.30 Mean Time Delay Errors Using P_i for Arrivals Described in Table 4.18

Method	Delay 1	Delay 2	Delay 3	Average
Analytical	0.0057	0.0758	0.0405	0.0407
Gibbs Sampling	0.0048	0.0755	0.0438	0.0414
MF	0.0056	0.0715	0.0637	0.0469
EM	0.0030	0.0574	0.0841	0.0482
SA	0.0222	0.1030	0.0672	0.0641

Table 4.31 Mean Amplitude Errors Using P_i for Arrivals Described in Table 4.18

Method	Delay 1	Delay 2	Delay 3	Average
Analytical	0.0043	0.0050	0.0040	0.0044
Gibbs Sampling	0.0045	0.0051	0.0043	0.0046
MF	0.0044	0.0058	0.0050	0.0051
EM	0.0030	0.0058	0.0045	0.0044
SA	0.0041	0.0063	0.0029	0.0044

4.2.1 EM Algorithm and Initial Conditions

The EM results were surprising to us. This led to some further investigation into the process. The algorithm was, thus, run one hundred times on the same signal, each time starting with a different randomly selected set of initial conditions. The assumption that EM's performance depends on the chosen initial condition was confirmed. However, as it will be shown in the results that follow the choice of initial conditions is not obvious. A two arrival problem was examined. The initial conditions for the first and second delays are given as well as the L_1 error for the initial conditions which resulted in estimates with the least error and the greatest error. Tables 4.41

Table 4.32 Mean L_1 and L_2 Errors for Arrivals Described in Table 4.22

Method	Mean L_1 Error	Mean L_2 Error
Analytical	0.0772	0.2141
Gibbs Sampling	0.0780	0.2131
MF	0.0816	0.2380
EM	0.1381	0.4804
SA	0.0881	0.2448

Table 4.33 Mean Time Delay Errors Using P_i for Arrivals Described in Table 4.22

Method	Delay 1	Delay 2	Delay 3	Average
Analytical	0.0143	0.0277	0.0217	0.0212
Gibbs Sampling	0.0139	0.0276	0.0216	0.0210
MF	0.0249	0.0287	0.0263	0.0266
EM	0.0652	0.0558	0.1216	0.0809
SA	0.0144	0.0341	0.0274	0.0253

through 4.46 are error results for signals with two arrivals. The correct delays are at 50 at 60 and their corresponding amplitudes are 100 and -90. The initial conditions are required to get the EM algorithm started. Changing these conditions greatly impacts the estimation process which we can see by the huge discrepancies in the errors. There is a big difference between the least and the greatest error which is calculated using the parameter estimates obtained by EM.

Using the stated initial conditions, the resulting estimates that correspond to the least L_1 errors, 0.00009 (for noise variance 0.01), 0.0055 (for noise variance 0.05), and 0.0060 (for noise variance 0.1) are presented in Table 4.41, Table 4.43, and Table

Table 4.34 Mean Amplitude Errors Using P_i for Arrivals Described in Table 4.22

Method	Delay 1	Delay 2	Delay 3	Average
Analytical	0.0045	0.0084	0.0053	0.0061
Gibbs Sampling	0.0043	0.0088	0.0062	0.0064
MF	0.0047	0.0071	0.0056	0.0058
EM	0.0030	0.0053	0.0035	0.0039
SA	0.0048	0.0104	0.0058	0.0070

Table 4.35 Mean L_1 and L_2 Errors for Arrivals Described in Table 4.18

Method	Mean L_1 Error	Mean L_2 Error
Analytical	0.1088	0.3084
Gibbs Sampling	0.1507	0.3535
MF	0.1589	0.5593
EM	0.1315	0.4865
SA	0.1339	0.4334

4.45, respectively. The greatest L_1 errors, 0.3671 (for noise variance 0.01), 0.3772 (for noise variance 0.05), and 0.3960 (for noise variance 0.1) are presented in Table 4.42, Table 4.44, and Table 4.46, respectively. It appears that the initial conditions chosen for the time delays is a critical factor responsible for EM's performance. In the examples presented, the error is maximized when the starting values for each delay approach the end of the received sequence. However, changing the initial conditions does not guarantee that the algorithm will converge to the true parameter values. In addition, if resources are expended in running the code for multiple sets of initial conditions, we argue that Gibbs sampling can be efficiently used in the first place.

Table 4.36 Mean Time Delay Errors Using P_i for Arrivals Described in Table 4.18

Method	Delay 1	Delay 2	Delay 3	Average
Analytical	0.0181	0.0930	0.0399	0.0503
Gibbs Sampling	0.0273	0.0977	0.0381	0.0544
MF	0.0941	0.1651	0.1149	0.1247
EM	0.0916	0.1252	0.1081	0.1083
SA	0.0470	0.1616	0.0337	0.0808

Table 4.37 Mean Amplitude Errors Using P_i for Arrivals Described in Table 4.18

Method	Delay 1	Delay 2	Delay 3	Average
Analytical	0.0168	0.0213	0.0086	0.0155
Gibbs Sampling	0.0498	0.0912	0.0375	0.0595
MF	0.0076	0.0147	0.0068	0.0097
EM	0.0058	0.0052	0.0031	0.0047
SA	0.0102	0.0110	0.0053	0.0088

As mentioned earlier, the results using EM on the two arrival problem with delays at 50 and 52 and corresponding amplitudes 100 and -90 are poor. Illustrated in Figures 4.11 and 4.12 is an example which is typical of the outcomes obtained from multiple runs of the algorithm for this signal. The initial conditions used are (49,105) for the first arrival and (53,-85) for the second arrival, seemingly ideal considering the true values. Figure 4.11 plots the samples at each iteration for the amplitude of the first delay and Figure 4.12 graphs the samples for the second delay. As the EM process runs, the samples diverge from the true amplitudes, in spite of the initial conditions and regardless of the length of time the code is allowed to run.

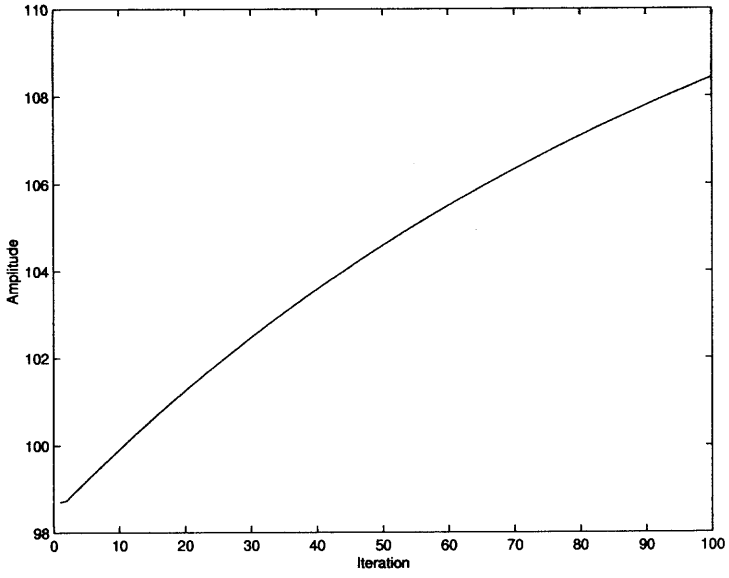

Figure 4.11 Samples obtained by EM for amplitude of the first arrival.

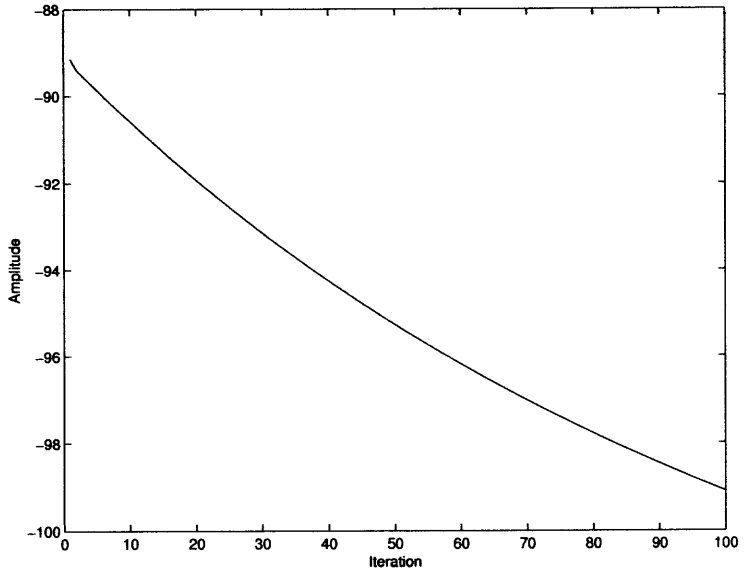

Figure 4.12 Samples obtained by EM for amplitude of the second arrival.

Table 4.38 Mean L_1 and L_2 Errors for Arrivals Described in Table 4.22

Method	Mean L_1 Error	Mean L_2 Error
Analytical	0.1085	0.2880
Gibbs Sampling	0.1046	0.2761
MF	0.1163	0.3177
EM	0.1470	0.4966
SA	0.1116	0.2960

Table 4.39 Mean Time Delay Errors Using P_i for Arrivals Described in Table 4.22

Method	Delay 1	Delay 2	Delay 3	Average
Analytical	0.0214	0.0420	0.0305	0.0313
Gibbs Sampling	0.0209	0.0378	0.0283	0.0290
MF	0.0388	0.0454	0.0335	0.0392
EM	0.0756	0.0666	0.1172	0.0865
SA	0.0276	0.0448	0.0307	0.0344

4.3 Gibbs Distributions

Point estimates obtained from Gibbs sampling through MAP estimation do not necessarily coincide with the true, unknown parameter values. That is particularly anticipated as a result of estimation with Gibbs sampling or any other method when the received signals are particularly noisy. As mentioned before, a beneficial feature incorporated in the Gibbs sampling algorithm is the computation of the posterior probability density functions of the unknown parameters. To emphasize the significance, we include Figure 4.13. Unlike the other algorithms, which only

Table 4.40 Mean Amplitude Errors Using P_i for Arrivals Described in Table 4.22

Method	Delay 1	Delay 2	Delay 3	Average
Analytical	0.0088	0.0124	0.0091	0.0101
Gibbs Sampling	0.0081	0.0128	0.0094	0.0101
MF	0.0084	0.0122	0.0092	0.0099
EM	0.0042	0.0060	0.0045	0.0049
SA	0.0088	0.0169	0.0059	0.0105

Table 4.41 L_1 Error Using the Given Initial Conditions for EM With Noise Variance 0.01

	Arrival 1 (Time,Amplitude)	Arrival 2 (Time,Amplitude)
Initial Condition	(42,-65)	(66,-46)
Estimate	(50,100)	(60,-80)

provide point estimates for each arrival, the Gibbs sampling algorithm allows us to view the distributions obtained for the time delays and amplitudes.

The true delays in this example are 10, 30 and 150. The point estimates for the time delays from Gibbs sampling are 10, 149, and 149. It appears that the algorithm was unable to find the second arrival at delay 30. Looking at the distribution, Figure 4.13, however, we can see that there another arrival at the appropriate delay (30).

The Gibbs sampling - maximum a posteriori estimation approach has demonstrated to be more informative than other time delay and amplitude estimation methods, because it provides a wider picture of the probability that unknown parame-

Table 4.42 L_1 Error Using the Given Initial Conditions for EM With Noise Variance 0.01

	Arrival 1 (Time,Amplitude)	Arrival 2 (Time,Amplitude)
Initial Condition	(199,81)	(199,-60)
Estimate	(197,69)	(198,-63)

Table 4.43 L_1 Error Using the Given Initial Conditions for EM With Noise Variance 0.05

	Arrival 1 (Time,Amplitude)	Arrival 2 (Time,Amplitude)
Initial Condition	(49,77)	(92,-81)
Estimate	(50,118)	(58,-91)

ters take on a broad range of values. Thus, information that would be concealed by the point estimates is now revealed.

The results presented in this chapter strongly support the argument in favor of using Gibbs sampling to estimate arrival times and amplitudes of signals. Overall the results found from the Gibbs sampler most resemble the optimal analytic results. Unlike the other methods presented for the comparison, Gibbs sampling is not affected by initial conditions chosen by the user, nor is it significantly affected by the sigal characteristics.

Table 4.44 L_1 Error Using the Given Initial Conditions for EM With Noise Variance 0.05

	Arrival 1 (Time,Amplitude)	Arrival 2 (Time,Amplitude)
Initial Condition	(199,98)	(199,-51)
Estimate	(191,119)	(191,-97)

Table 4.45 L_1 Error Using the Given Initial Conditions for EM With Noise Variance 0.1

	Arrival 1 (Time,Amplitude)	Arrival 2 (Time,Amplitude)
Initial Condition	(39,89)	(129,39)
Estimate	(50,120)	(58,-88)

Table 4.46 L_1 Error Using the Given Initial Conditions for EM With Noise Variance 0.1

	Arrival 1 (Time,Amplitude)	Arrival 2 (Time,Amplitude)
Initial Condition	(177,102)	(184,-79)
Estimate	(191,179)	(191,-148)

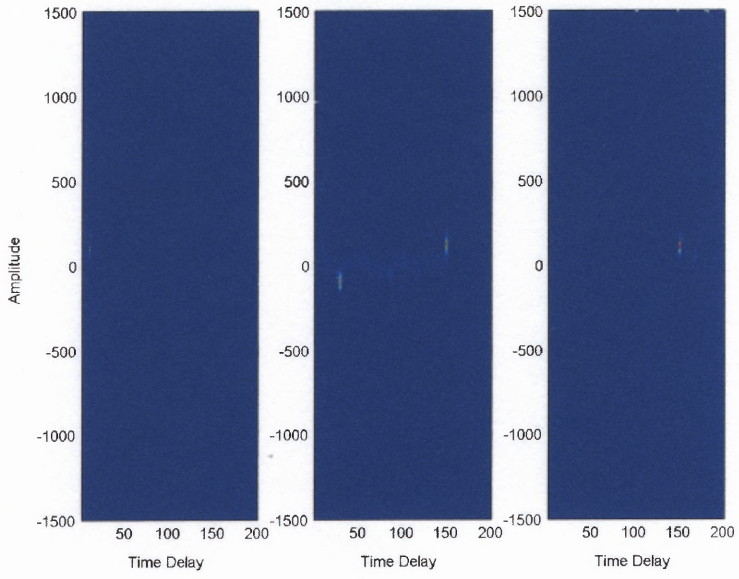

Figure 4.13 Distributions obtained by Gibbs sampling.

CHAPTER 5

MODELLING VARIANCE AS AN UNKNOWN PARAMETER

Recall that the received signal follows Equation (1.1). We have shown that the Gibbs sampler successfully identified the amplitudes and time delays assuming the noise variance was known. This variance is now treated as an unknown parameter, added to the attenuated and delayed replicas of the transmitted signal. To do this, we make use of the following theorem:

Thm.: Let the sample quantity s^2 be distributed as $(\sigma^2/N)\chi^2_N$. If the prior distribution of $log\sigma$ is locally uniform, then, given s^2, σ^2 is distributed a posteriori as $(Ns^2)\chi_N^{-2}$ [34].

In the context of the work presented here, χ^2_N is the sum of the squares of N random numbers. N is the length of the received signal and $Ns^2 = \sum_{n=1}^{N}(r(n) - \sum_{i=1}^{M} a_i s(n-n_i))^2$

We will use the following noninformative prior for the variance [30, 34].

$$p(\sigma^2) = \frac{1}{\sigma^2}, \quad \sigma^2 > 0 \tag{5.1}$$

This choice represents the fact that no information is available on the variance. Including this in the joint distribution Equation 3.5, we can now write the posterior probability distribution function of all unknown parameters (in this case, n_i, a_i for $i = 1, \ldots, M$, and σ^2) as follows:

$$p(n_1, ..., n_M, a_1, ..., a_M, \sigma^2 | r(n)) =$$
$$H \frac{1}{N^M} \frac{1}{\sigma^2} \frac{1}{(\sqrt{2\pi})^N \sigma^N} exp(-\frac{1}{2\sigma^2} \sum_{n=1}^{N} (r(n) - \sum_{i=1}^{M} a_i s(n-n_i))^2), \tag{5.2}$$

where H is a constant.

Consolidating all the constants in Equation 5.2, the conditional distribution of σ^2 given a_i and n_i, $i = 1, 2, ..., M$ and received signal $r(n)$ can be written as:

$$p(\sigma^2|n_i, a_i, r(n)) = F\frac{1}{\sigma^{N+2}}exp(-\frac{1}{2\sigma^2}\sum_{n=1}^{N}(r(n) - \sum_{i=1}^{M} a_i s(n - n_i))^2). \quad (5.3)$$

F is the normalizing constant of the distribution.

This conditional distribution is recognized as a chi-square distribution with N degrees of freedom, χ^2_N. Equation 5.3 is used to generate samples variance.

5.1 Results for Unknown Variance

Treating the noise variance as an unknown parameter in the Gibbs sampling algorithm, samples were obtained using Equation 5.3. Synthetic data was constructed for the source shown in Figure 5.1. The results are presented for received signals with time delays and amplitudes included in Tables 5.1 and 5.2. Three different noise variances are considered, .01, .05 and .1. Figures 5.2 - 5.4 show the noisy realizations of the received signal for the three cases.

Table 5.1 True Values for the Wide Arrival Case

Arrival	Time delay	Amplitude
1	10	100
2	30	-80
3	150	60

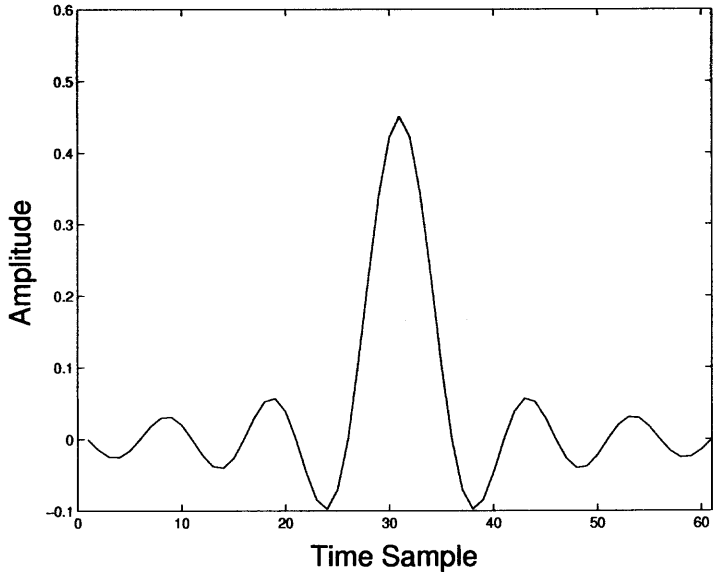

Figure 5.1 Source signal.

Table 5.2 True Values for the Close Arrival Case

Arrival	Time delay	Amplitude
1	10	100
2	15	-80
3	150	60

Figures 5.5 through 5.7 present samples of the posterior distributions of the variance as obtained from the Gibbs sampler for the wide arrival case for the indicated. The results presented show Gibbs sampling's overwhelming ability to correctly identify the variance.

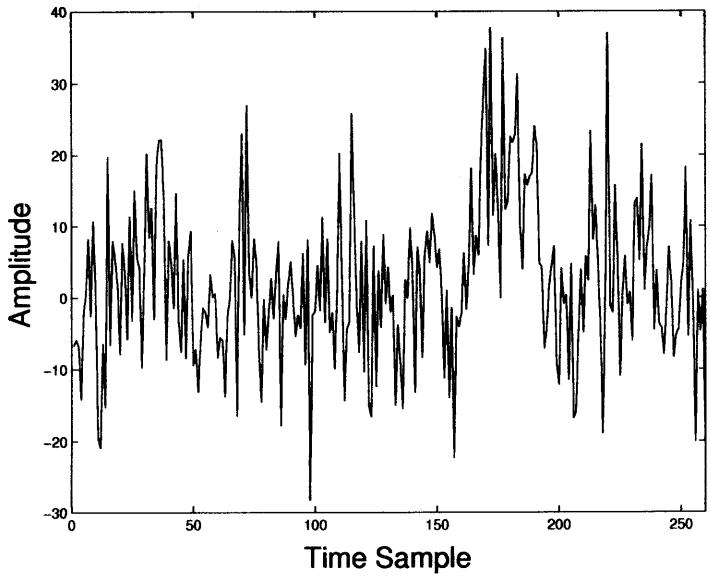

Figure 5.2 Signal obtained at the receiver for three arrivals widely spaced with noise variance 0.01.

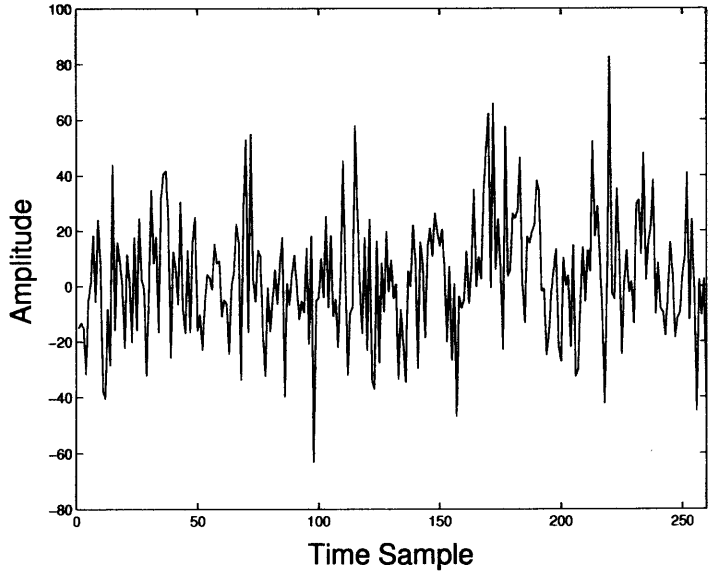

Figure 5.3 Signal obtained at the receiver for three arrivals widely spaced with noise variance 0.05.

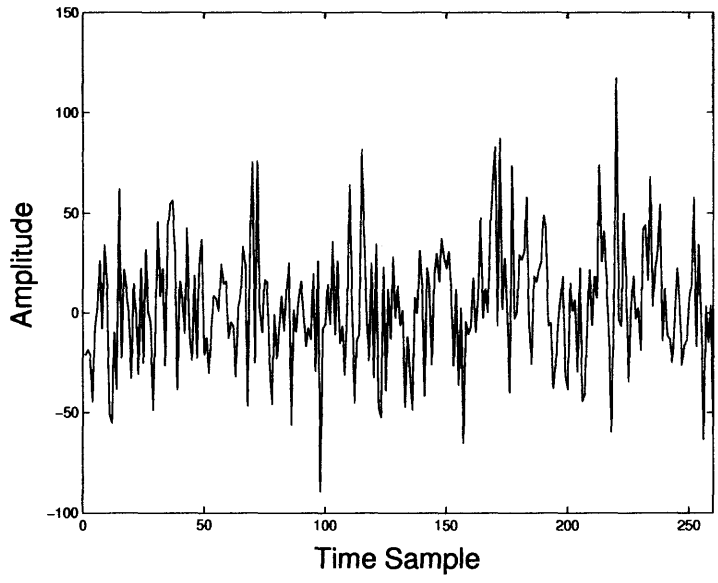

Figure 5.4 Signal obtained at the receiver for three arrivals widely spaced with noise variance 0.1.

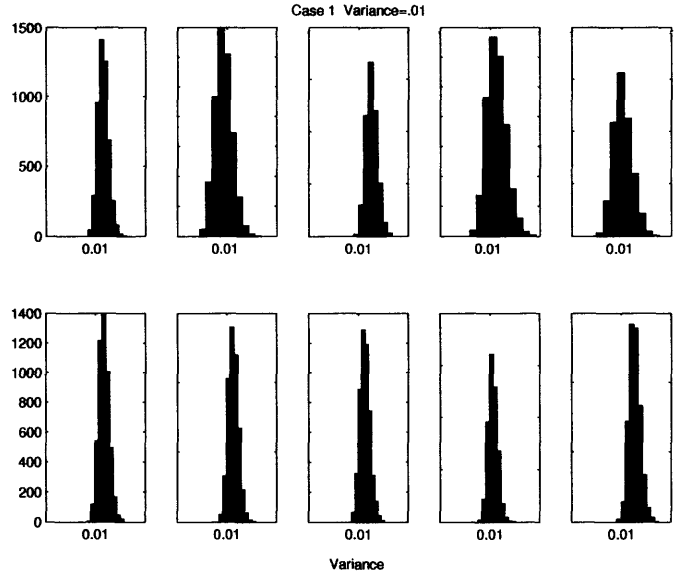

Figure 5.5 Distributions for the variance obtained from 10 runs of the Gibbs sampling algorithm for the wide arrival signal. The true variance is 0.01.

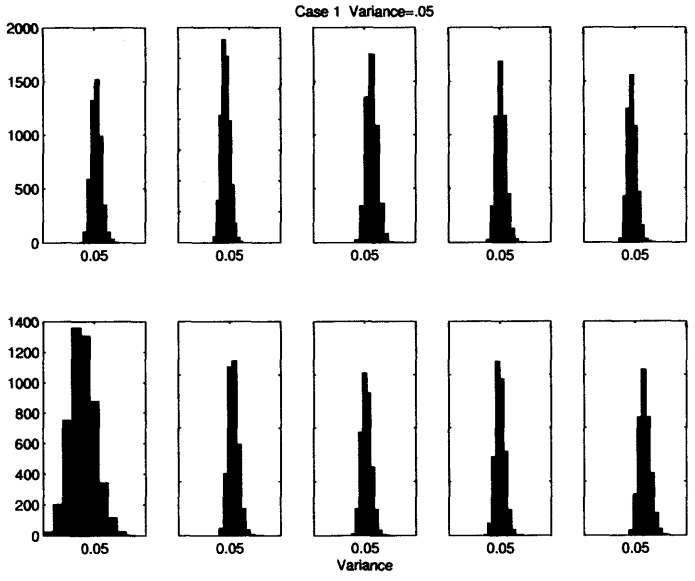

Figure 5.6 Distributions for the variance obtained from 10 runs of the Gibbs sampling algorithm for the wide arrival signal. The true variance is 0.05.

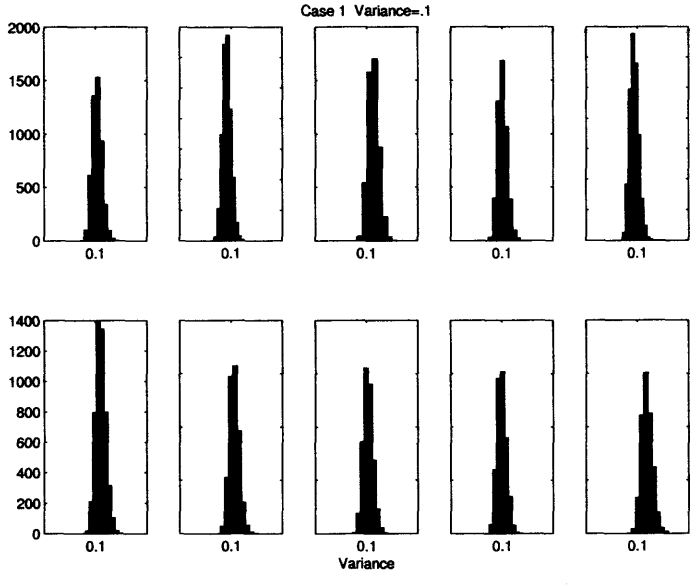

Figure 5.7 Distributions for the variance obtained from 10 runs of the Gibbs sampling algorithm for the wide arrival signal. The true variance is 0.1.

Figures 5.8 through 5.10 present variance samples for the close arrival case for the indicated noise variances.

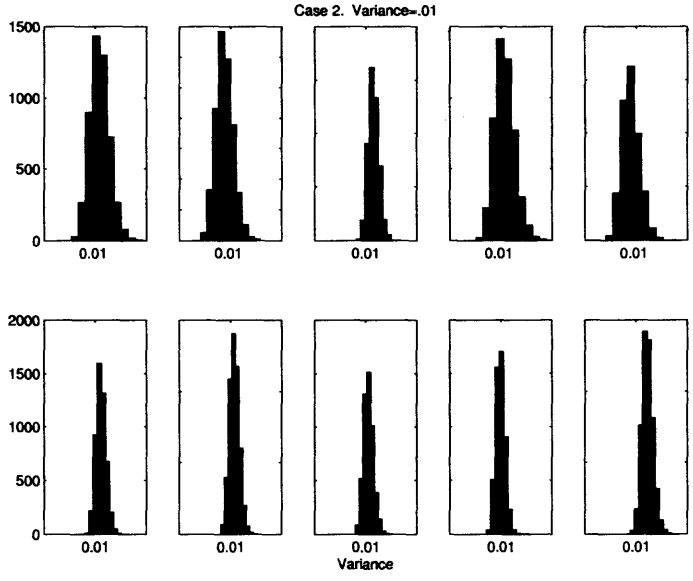

Figure 5.8 Distributions for the variance obtained from 10 runs of the Gibbs sampling algorithm for the close arrival signal. The true variance is 0.01.

5.2 Importance of Accurate Variance Estimation

The following graphs show the importance of correctly estimating the noise variance and the effects of an assumption of a wrong variance on the arrival estimates. When the assumed variance is correct as in Figure 5.11 the Gibbs sampler appears to be able to find the arrivals with more certainty than when the incorrect variance is considered, Figure 5.12. Using the Gibbs sampler to estimate the variance actually improves the performance of the algorithm in estimating the arrivals. When the noise is incorrectly estimated, there is more ambiguity in the distributions and hence, decreases the likelihood the time delays and amplitudes will be estimated accurately.

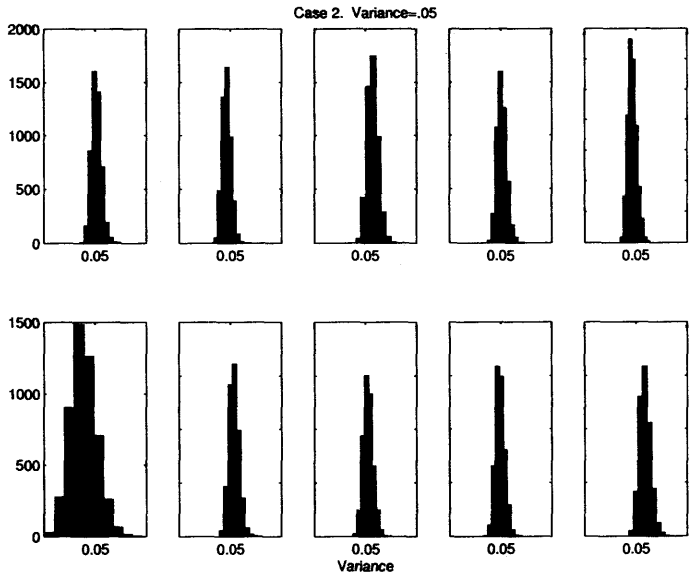

Figure 5.9 Distributions for the variance obtained from 10 runs of the Gibbs sampling algorithm for the close arrival signal. The true variance is 0.05.

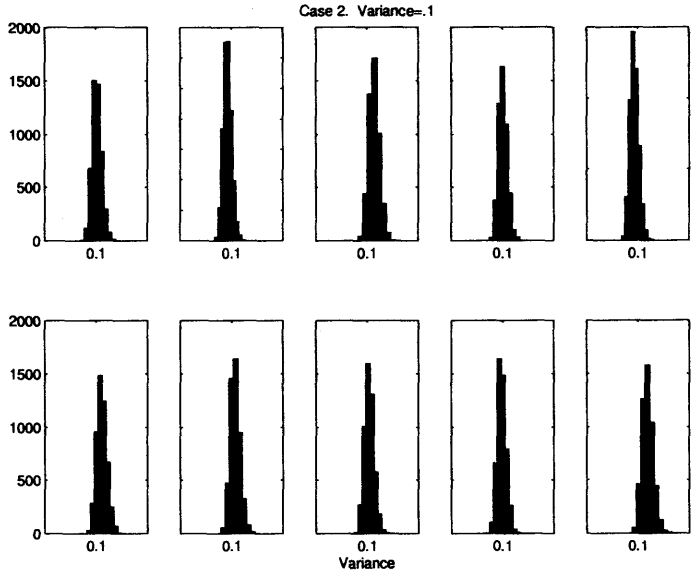

Figure 5.10 Distributions for the variance obtained from 10 runs of the Gibbs sampling algorithm for the close arrival signal. The true variance is 0.1.

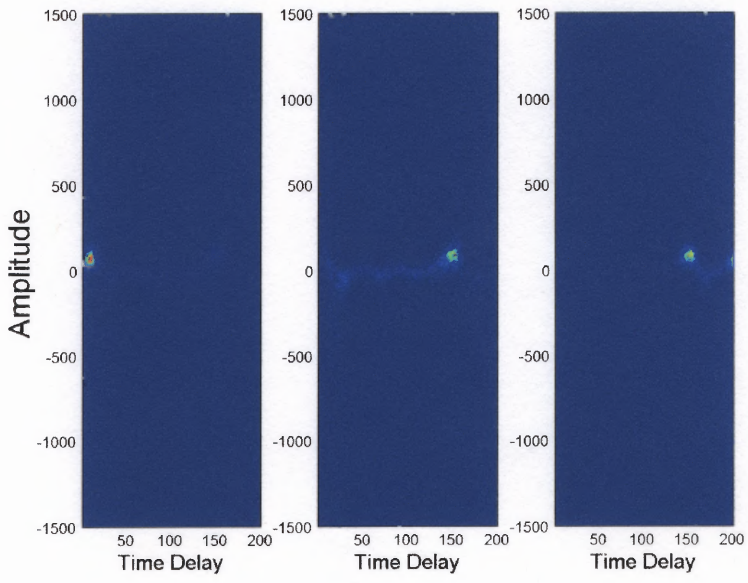

Figure 5.11 Time delay and amplitude distributions obtained by Gibbs sampling assuming the true variance.

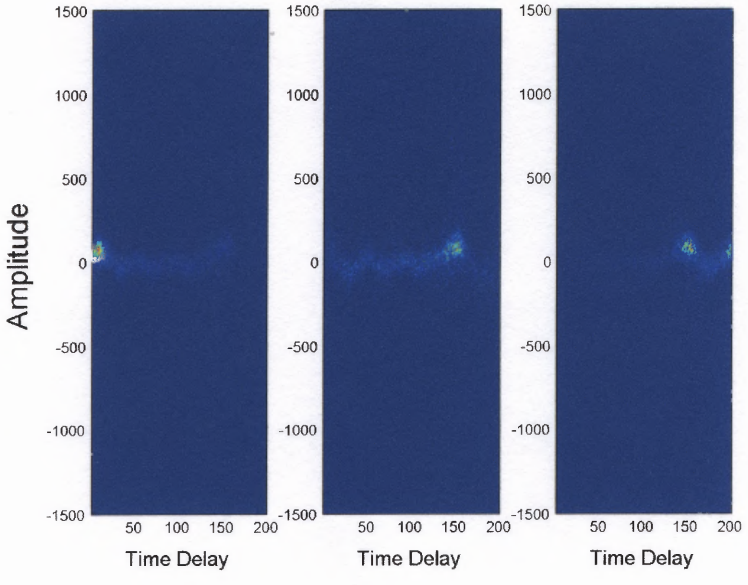

Figure 5.12 Time delay and amplitude distributions obtained by Gibbs sampling assuming a wrong variance of 0.1 (true variance is 0.05).

CHAPTER 6

UNKNOWN NUMBER OF ARRIVALS

We have assumed until now that the number of arrivals in the received signal is known. This assumption is quite common [17, 35]. It is argued that this is not as restrictive as it appears since, in many cases the number of paths (arrivals) can be determined from the geometry of the channel. However, since we do not assume any prior knowledge about the environment, it is not valid to assume prior knowledge about the number of arrivals. Therefore, the next task at hand is to use the Gibbs sampling algorithm to determine the number of arrivals present in the received signal.

6.1 Empirical Approach

First, we run the Gibbs sampling algorithm assuming present in the received signal are two arrivals, three arrivals, four arrivals, etc. One interesting feature of the Gibbs sampler is that, when generating samples for the time delays, the program can be forced to find an arrival different from those already found. When running the Gibbs sampler assuming the number of arrivals is greater than the true number of arrivals, the process often gets "stuck" in a loop. This is the first indication that the original guess exceeds the true number of arrivals and provides a limit on the maximum number of arrivals that should be assumed when running the algorithm. Exploiting this phenomenon, we can implement a flag waving technique suggesting that it may be necessary to reduce the assumed number of arrivals.

Furthermore, we can study the distributions obtained for each considered case. In the next example, the true number of arrivals is three. The received time-series is generated employing the source signal of Figure 6.1 with various amplitudes, time delays, and added noise.

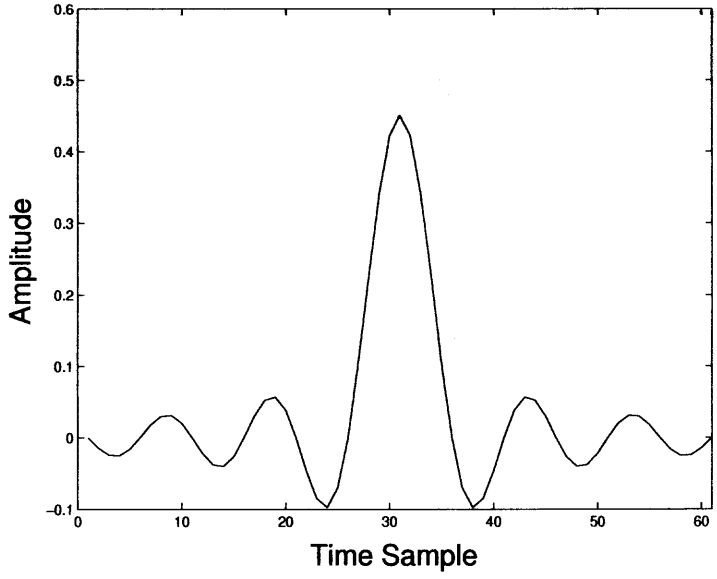

Figure 6.1 Source signal.

Figures 6.2 through 6.4 present time delay and amplitude distributions for the received signal with arrivals given in Table 6.1 and noise variance 0.01.

Table 6.1 True Values for the Wide Arrival Case

Arrival	Time delay	Amplitude
1	10	100
2	30	-80
3	150	60

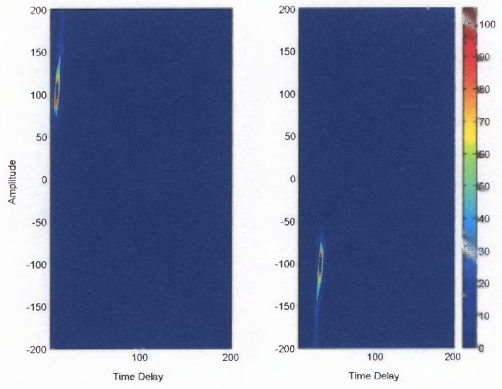

Figure 6.2 Distributions obtained by Gibbs sampling assuming two arrivals are present for the wide arrival signal with variance 0.01.

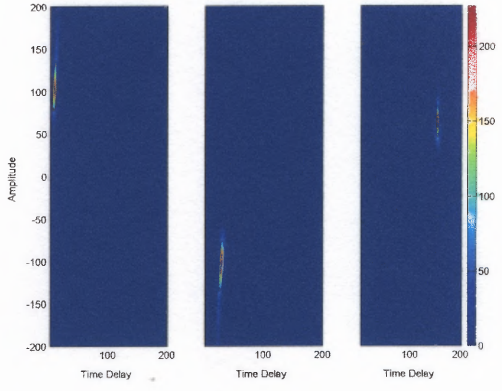

Figure 6.3 Distributions obtained by Gibbs sampling assuming three arrivals are present for the wide arrival signal with variance 0.01.

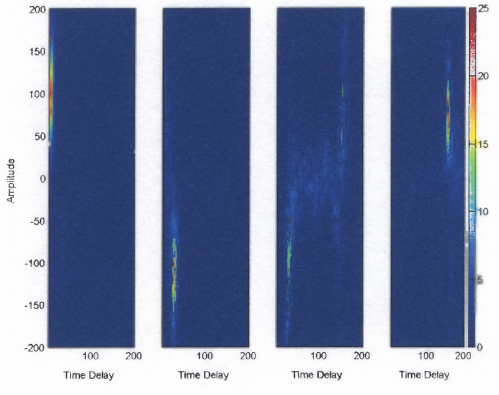

Figure 6.4 Distributions obtained by Gibbs sampling assuming four arrivals are present for the wide arrival signal with variance 0.01.

Figure 6.2 demonstrates the distributions obtained from Gibbs sampling assuming that the signal consists of two arrivals. The algorithm correctly identifies the first two. Figure 6.3 plots the Gibbs distributions assuming three arrivals are present. We can clearly identify a third, distinct arrival not located in the previous trial. Continuing on, Figure 6.4 displays the distributions obtained when the Gibbs sampling algorithm is prompted to find four arrivals. The four subplots in Figure 6.4 are the individual distributions for each arrival (that is, these are joint distributions of arrival time and amplitude). We can see that there is ambiguity in the third subplot. The algorithm does not find a distinct arrival, instead, sometimes it identifies the true second arrival and other times it locates the true third arrival. The extra arrival seems to be a duplicate of a true arrival. Looking at these graphs, there is a strong indication that there truly are only three arrivals present. Notice that the algorithm not only finds the correct number of arrivals but also correctly identifies the arrival times.

Figures 6.5 through 6.7 are the distributions for the received signal with arrivals given in Table 6.1 and variance of noise 0.05. These distributions are quite similar to the respective distributions obtained in the previous example. Therefore, we again conclude the algorithm success- fully estimates the correct number of arrivals.

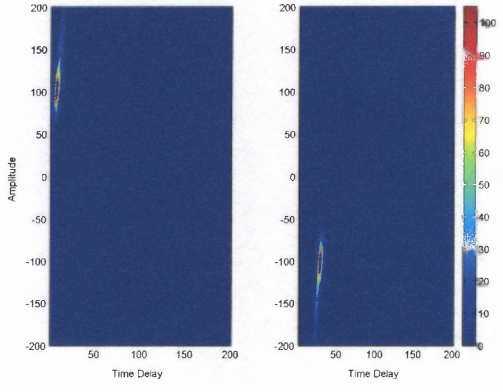

Figure 6.5 Distributions obtained by Gibbs sampling assuming two arrivals are present for the wide arrival signal with variance 0.05.

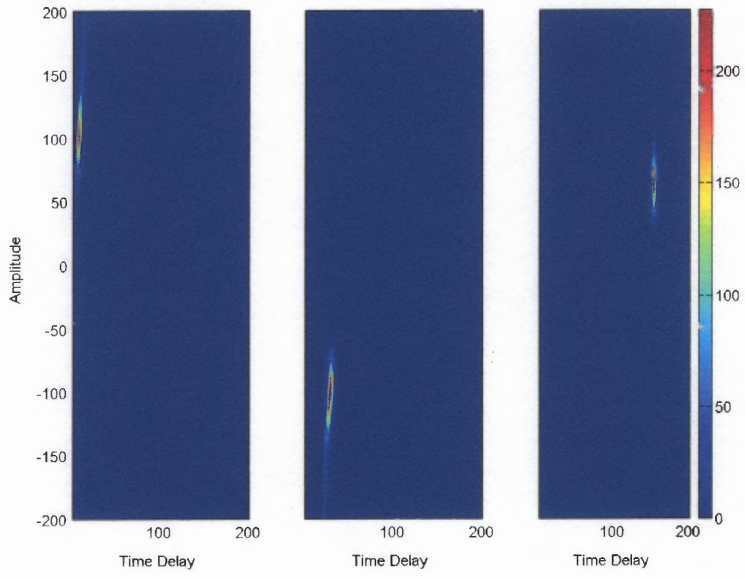

Figure 6.6 Distributions obtained by Gibbs sampling assuming three arrivals are present for the wide arrival signal with variance 0.05.

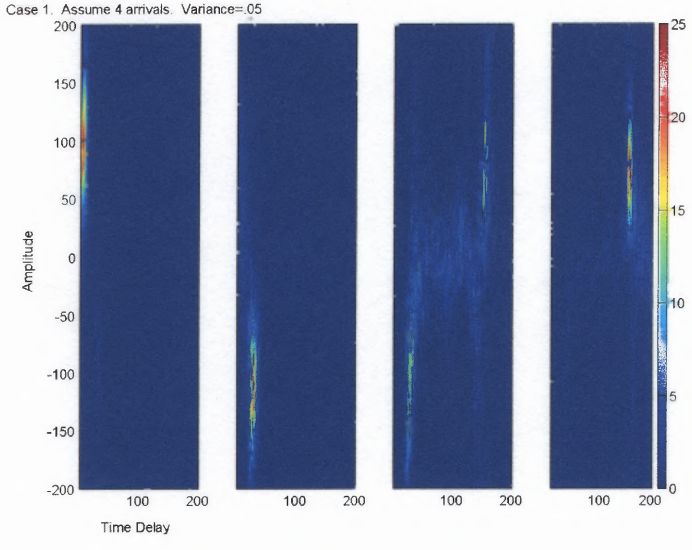

Figure 6.7 Distributions obtained by Gibbs sampling assuming four arrivals are present for the wide arrival signal with variance 0.05.

Figures 6.8 through 6.10 are the distributions for the received signal with arrivals given in Table 6.1 and variance of noise 0.1.

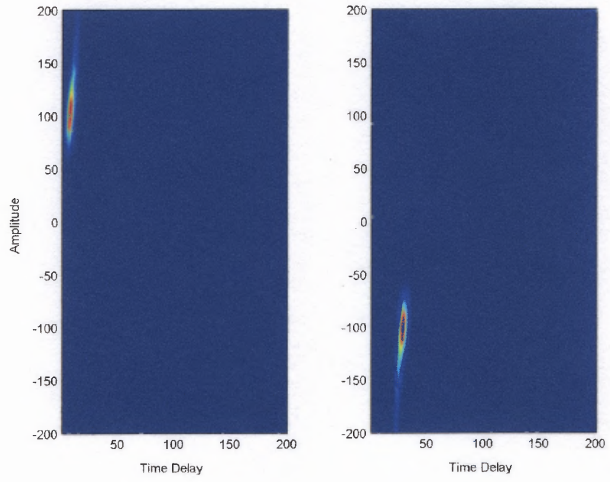

Figure 6.8 Distributions obtained by Gibbs sampling assuming two arrivals are present for the wide arrival signal with variance 0.1.

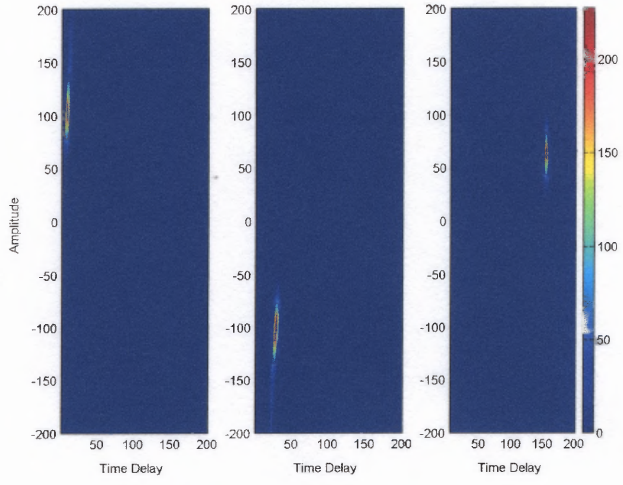

Figure 6.9 Distributions obtained by Gibbs sampling assuming three arrivals are present for the wide arrival signal with variance 0.1.

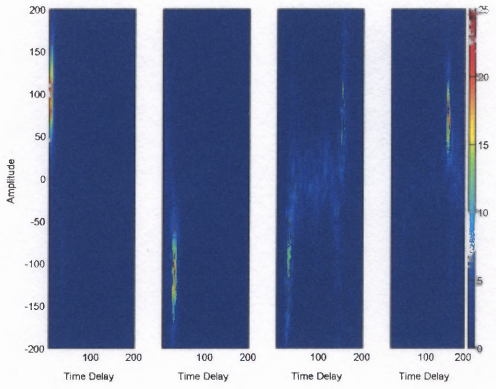

Figure 6.10 Distributions obtained by Gibbs sampling assuming four arrivals are present for the wide arrival signal with variance 0.1.

6.2 Analytic Approach

The next step is to mathematically formulate the behavior observed in the previous section. This can be done using techniques similar to Akaike Information Criteria (AIC) and Schwartz [36], approaches typically employed to determine the number of parameters involved in a problem. In essence, the AIC approach involves the log-likelihood of the maximum likelihood estimator of the parameters of the model. Whereas, Schwartz's approach is based on Bayesian arguments; assume that each competing model can be assigned a prior probability, and select the model which yields the maximum posterior probability. Samples are generated for the posterior distributions of the time delays, amplitudes, and noise variance using the Gibbs sampler, assuming various numbers of arrivals are present.

We will use the following uniform prior for the number of arrivals M:

$$p(M) = \frac{1}{Q}, \tag{6.1}$$

where $Q = M_{max} - M_{min} + 1$.

This choice represents the fact that no information is available on the number of arrivals. However, whenever possible, prior knowledge indicating the maximum

number of arrivals should be taken into consideration to avoid unnecessary calculations. The conditional probability of all unknown parameters (in this case, n_i, a_i for $i = 1, \ldots, M$, and, σ^2) given the number of arrivals M and a received signal $r(n)$can be written as follows:

$$p(n_1, ..., n_M, a_1, ..., a_M, \sigma^2 | M, r(n)) =$$
$$K \frac{1}{N^M} \frac{1}{(\sqrt{2\pi})^N \sigma^N} exp(-\frac{1}{2\sigma^2} \sum_{n=1}^{N} (r(n) - \sum_{i=1}^{M} a_i s(n - n_i))^2), \tag{6.2}$$

where $1/K$ is the N-dimensional joint probability density function of $r(n)$, $n = 1, ..., N$, which is a constant.

Marginal distribution of M given a received signal is obtained by integrating the product of Equation 6.2 and the prior for M over all unknowns. That is,

$$p(M|r(n)) = \int_{\sigma^2} \int_{a_1} \int_{a_2} \cdots \int_{a_M} \int_{n_1} \int_{n_2} \cdots \int_{n_M}$$
$$p(n_1, ..., n_M, a_1, ..., a_M, \sigma^2 | M, r(n)) p(M) dn_M ... dn_2 dn_1 da_M ... da_2 da_1 d\sigma^2 \tag{6.3}$$

In practice, the distribution of Equation 6.3 is obtained by first generating samples for the delays, amplitudes, and noise variance for a set of predetermined number of arrivals. The integral must be evaluated for all samples generated. Posterior distribution, $p(M|r(n))$, for the number of arrivals is then numerically implemented by summing the integrand in Equation 6.3 over all parameters.

6.3 Analytical Results for Unknown Number of Arrivals

Gibbs sampling was used to generate samples for the distributions of time delays and amplitudes for ten received signals with three different variances, 0.01, 0.05, and 0.1. The correct number of arrivals, delays, and amplitudes are shown in Tables 5.1 and 5.2. We ran the algorithm three different times assuming two arrivals, three arrivals, and four arrivals are present. This provided samples for the time delays

Table 6.2 Probability of Number of Arrivals for the Wide Arrival Case With Given Variance

Variance	2 Arrivals	3 Arrivals	4 Arrivals
0.01	3.7552x10^{-5}	0.9998	1.758x10^{-4}
0.05	0.0684	0.9306	0.0011
0.1	0.0243	0.9751	6.5071x10^{-4}

and amplitudes for each arrival, as well as the variance of noise. The modes of the distributions were used in Equation 6.3 to obtain a probability for each case of assumed number of arrivals.

The results presented in Table 6.2 and Table 6.3 are the mean probabilities for the ten widely spaced signals and ten closely spaced signals, respectively, for the assumed number of arrivals.

Figure 6.11 plots the mean probabilities using Equation 6.3, for ten received signals. Presented are the results for the received signal with variance of noise 0.05 for the widely spaced example shown in Table 5.1.

Table 6.3 Probability of Number of Arrivals for the Close Arrival Case With Given Variance

Variance	2 Arrivals	3 Arrivals	4 Arrivals
0.01	3.76x10^{-5}	0.9997	1.76x10^{-4}
0.05	0.08	0.919	0.01x10^{-1}
0.1	0.03	0.9693	6.51x10^{-4}

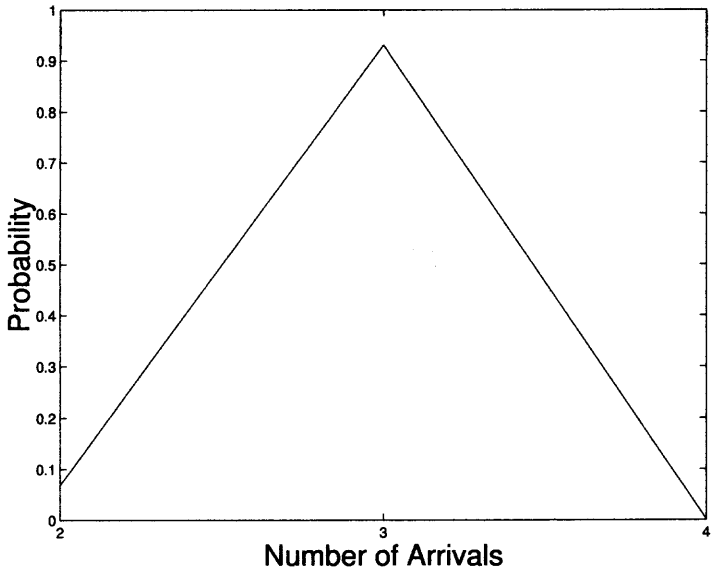

Figure 6.11 Mean probability for the given number of arrivals.

In both cases, for all amounts of noise, there was overwhelming success with the Gibbs sampler in being able to identify the correct number of arrivals.

CHAPTER 7

CONVERGENCE

When performing parameter estimation using iterative sampling-based techniques such as the Gibbs sampler, convergence must be monitored. Convergence of the samples generated from the proposed Gibbs sampling algorithm will be measured in two ways. First, the algorithm will be replicated with different starting points; it will then be checked whether the different runs converge to the same point (or, if not, we will note multiple solutions). In principle, the choice of starting values is unimportant since the Gibbs sampler should run long enough to "forget" its initial states. Early in the Gibbs process sampling in low probability regions is permitted, allowing it to move around the sample space [24, 28]. It is always useful to simulate at least two parallel sequences and examine the independent simulations to see if they converge. Experience suggests that with Bayesian posterior simulation, the added information obtained from replication out- weighs any additional costs required in multiple simulations. Then, we will also monitor the stability of the modes of the estimated distributions as a function of iteration number.

7.1 Convergence of Parallel Sequences

Figures 7.1 - 7.6 show the samples obtained at each iteration for the time delays and amplitudes for the signal presented in Table 5.1 (variance 0.01). The five plots in each figure are the results obtained for the given parameter from five runs of the Gibbs sampling algorithm. For each run, different initial conditions were chosen. The number of iterations was 5000 for each run. In practice, the number of iterations necessary before convergence is observed will vary. It depends on the signal; signals with high SNR require fewer iterations than signals with a lot of noise.

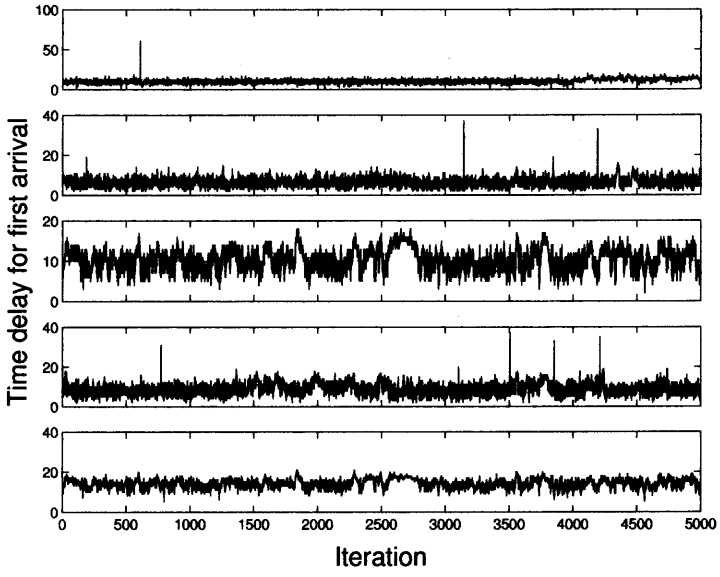

Figure 7.1 Samples for the time delay for the first arrival at each iteration.

Figure 7.1 presents the samples obtained at each iteration from the Gibbs sampling algorithm for the first delay. The true value is 10. It appears that the Gibbs sampler quickly converges to the correct time delay for the first arrival in all five runs.

Figure 7.2 demonstrates the samples obtained at each iteration using Gibbs sampling for the second delay. The true value is 30. In all five runs it appears that the Gibbs sampling algorithm converges to the correct time delay for the second arrival, as well.

Figure 7.3 contains the samples from five runs of the Gibbs sampling algorithm for the third delay. The true value is 150. Again convergence is observed.

Similarly, amplitude information is presented in Figures 7.4 - 7.6. The amplitudes are concentrated around the true values of 100, -80, and 60.

7.2 Convergence to a Distribution

Since convergence of the Gibbs sampling algorithm is really convergence to a distribution rather than to a point, it is reasonable to check convergence of the algorithm

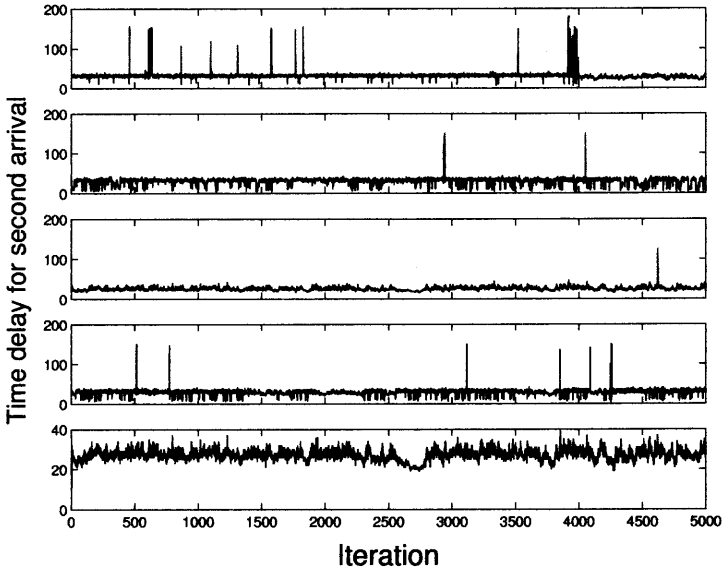

Figure 7.2 Samples for the time delay for the second arrival at each iteration.

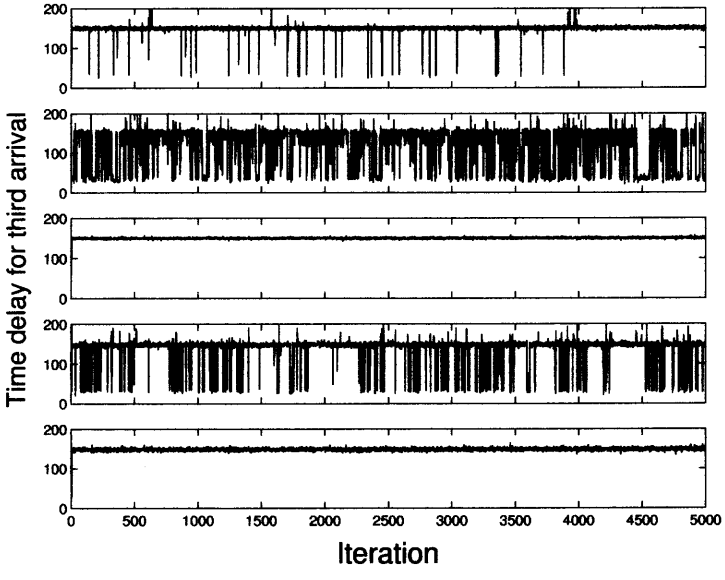

Figure 7.3 Samples for the time delay for the third arrival at each iteration.

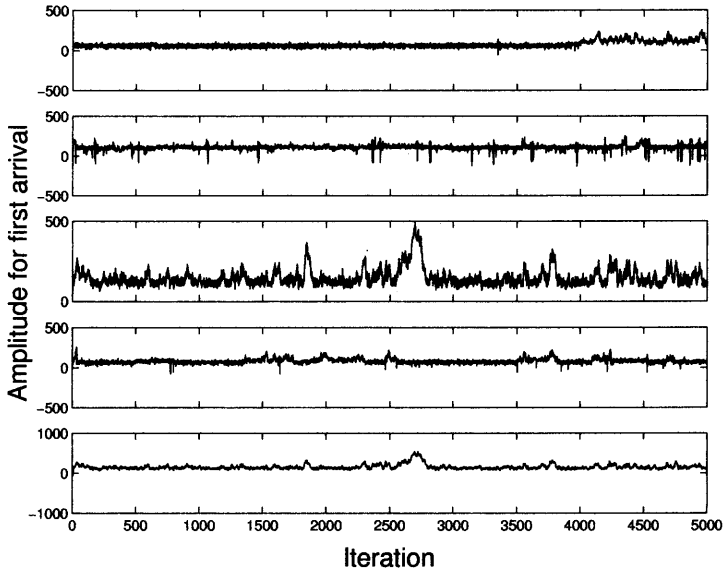

Figure 7.4 Samples for the amplitude for the first arrival at each iteration.

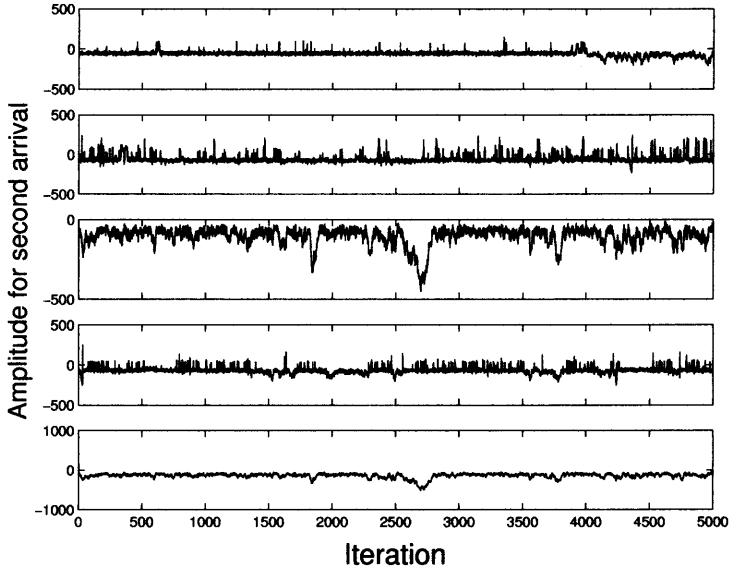

Figure 7.5 Samples for the amplitude for the second arrival at each iteration.

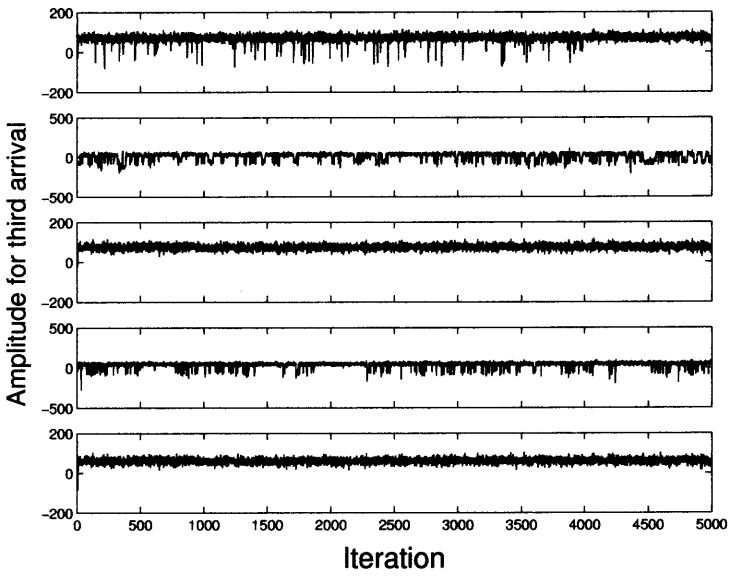

Figure 7.6 Samples for the amplitude for the third arrival at each iteration.

by looking at the modes of the distributions, the amplitudes and delays at which the distributions are maximized. To illustrate the algorithm's performance in this capacity, we will take a couple of different approaches.

To check convergence of a single run of the Gibbs sampling algorithm, we find the modes of the distributions obtained at various points throughout the iterative process. After throwing away the first 1000 samples, we find the modes for the second set of 1000 samples, the third set of 1000 samples, the fourth set of 1000 samples, and the fifth set of 1000 samples (for a run consisting of 5000 iterations). Presented here are the results for the amplitudes since, most often, if there is an issue of divergence, it is more prominent with the amplitudes. The estimates for the amplitudes of the first three arrivals are the modes for each distribution containing 1000 samples. The modes for each arrival correspond to the combination of amplitude and delay at which we observe the highest posterior probability.

Table 7.1 and Table 7.2 shows the results obtained for two different runs of Gibbs sampling. Each run is 5000 iterations long. The modes are calculated for each

distribution produced by the samples generated during the given iterations. The true amplitudes for the first, second, and third arrival are 100, -80 and 60, respectively.

Table 7.1 The Modes of the Amplitudes for Run 1

Iterations	A_1	A_2	A_3
1001-2000	95	-85	65
2001-3000	105	-75	55
3001-4000	95	-75	55
4001-5000	105	-85	55

Table 7.2 The Modes of the Amplitudes for Run 2

Iterations	A_1	A_2	A_3
1001-2000	95	-75	65
2001-3000	95	-85	65
3001-4000	95	-85	65
4001-5000	105	-85	65

Both runs of the algorithm converge to the correct modes for all three amplitudes very quickly.

To check whether the distributions obtained from different runs of the Gibbs sampler converge to the same mode, Table 7.3 presents the modes obtained for the amplitudes for each arrival for five runs. Each run is started with different initial conditions.

Table 7.3 The Modes of the Amplitudes for Five Different Runs

Run	A_1	A_2	A_3
1	95	-75	65
2	105	-85	55
3	105	-75	55
4	95	-85	65
5	95	-75	65

The results obtained from all five runs of the algorithm allow us to say, with a sufficient amount of confidence, that the correct estimates for the three amplitudes have been found.

7.3 Divergence Issues

It has also happened that a single run of Gibbs sampling appears to have "converged", but plots obtained from independent runs of the algorithm show that they are not converging to the same value. Figure 7.7 plots the samples obtained from two runs of Gibbs sampling for the time delay of the first arrival. The correct delay is 10. In the first plot, the value that appears the most is 6. In the second plot, this value appears to be 13. This emphasizes the benefits obtained from multiple runs of the Gibbs sampler. In situations like this, the inconsistencies can be remedied in several ways. The algorithm can be restarted using different initial conditions or the algorithm can continue to run longer. Using either approach, the algorithm will eventually converge to the same distribution.

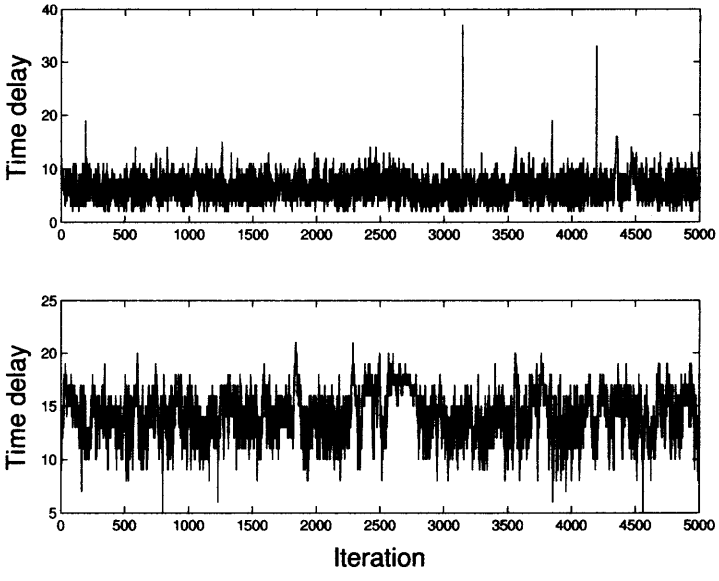

Figure 7.7 Samples obtained by Gibbs sampling for the time delay for the first arrival.

The Gibbs sampling algorithm does not necessarily converge quickly. It can happen that the user's choice of number of iterations may be insufficient to guarantee convergence. In our problem the number of iterations is typically set to 5000. Figures 7.8 and 7.9 present a case where divergence was detected within the first 5000

iterations. The process was then continued for an additional 5000 iterations, during which convergence to the true amplitude values of 100 and -80 was attained.

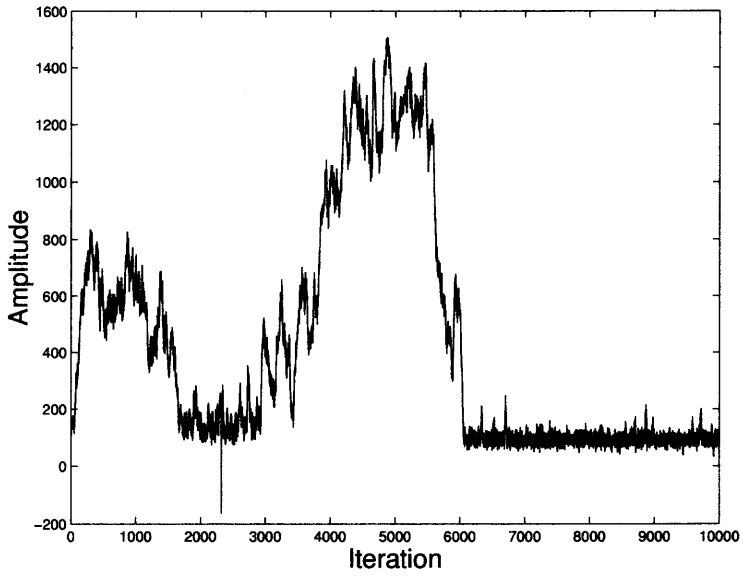

Figure 7.8 Samples obtained by Gibbs sampling for the amplitude for the first arrival at each iteration. The correct amplitude is 100.

As previously mentioned, another alternative to dealing with results that have diverged is to restart the program with a new seed, which is comparable to changing the initial conditions. This changes the values of the random variables generated at each iteration and, in turn, changes the samples generated. Figures 7.10 and 7.11 are the samples obtained for the amplitudes of the first and second arrivals, which have diverged.

Figures 7.12 and 7.13 are the samples obtained for the amplitudes of the first and second arrivals, which have now converged after rerunning the code with a new seed.

We can also see this trend by looking at the modes of the estimated distributions at various intervals throughout the iterative process. The modes are calculated for each distribution produced by the samples generated during a chosen set of iterations.

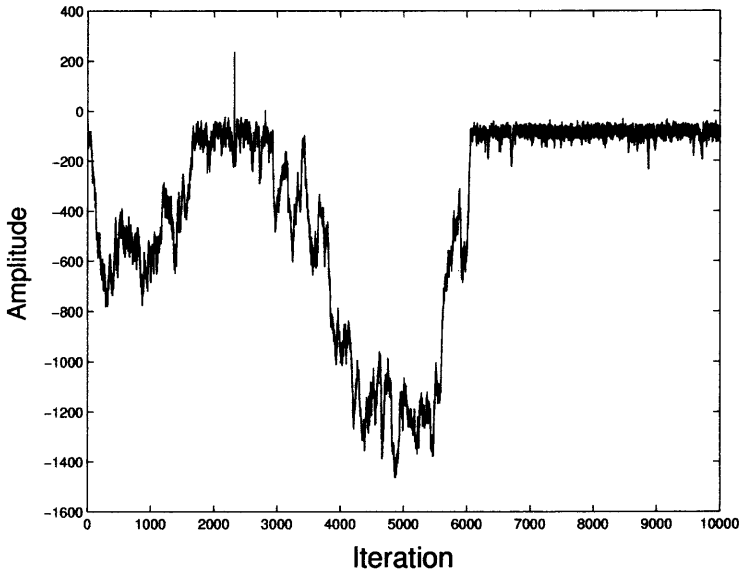

Figure 7.9 Samples obtained by Gibbs sampling for the amplitude for the second arrival at each iteration. The correct amplitude is -80.

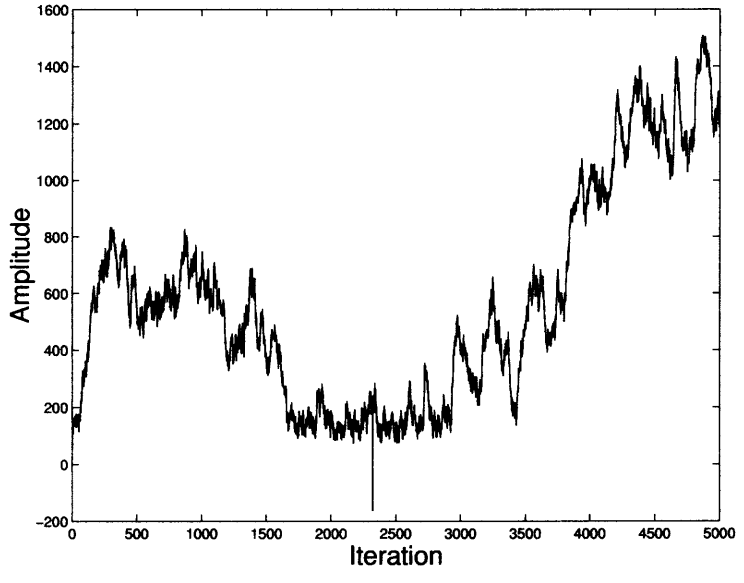

Figure 7.10 Samples obtained by Gibbs sampling for the amplitude for the first arrival at each iteration. The correct amplitude is 100.

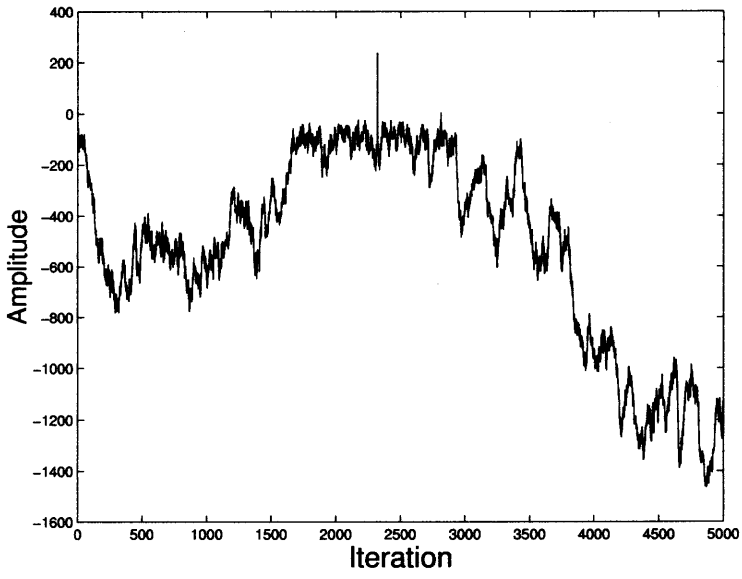

Figure 7.11 Samples obtained by Gibbs sampling for the amplitude for the second arrival at each iteration. The correct amplitude is -80.

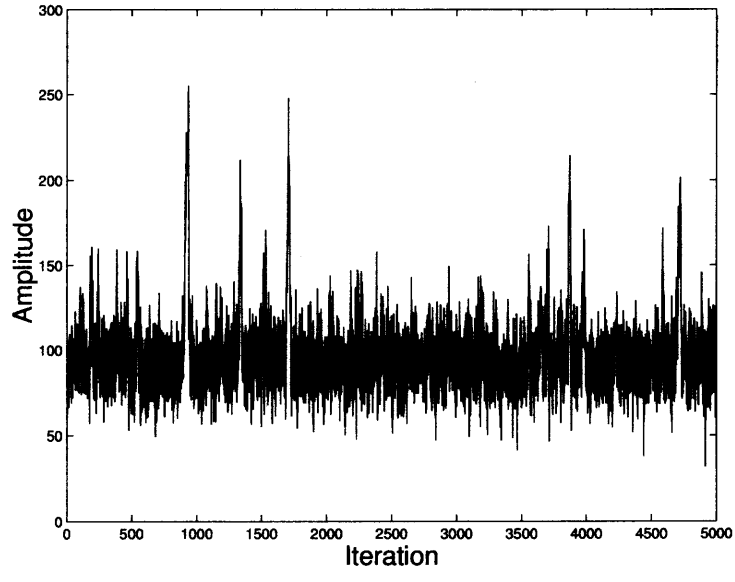

Figure 7.12 Samples obtained by Gibbs sampling for the amplitude of the first arrival vs. iteration. The correct amplitude is 100.

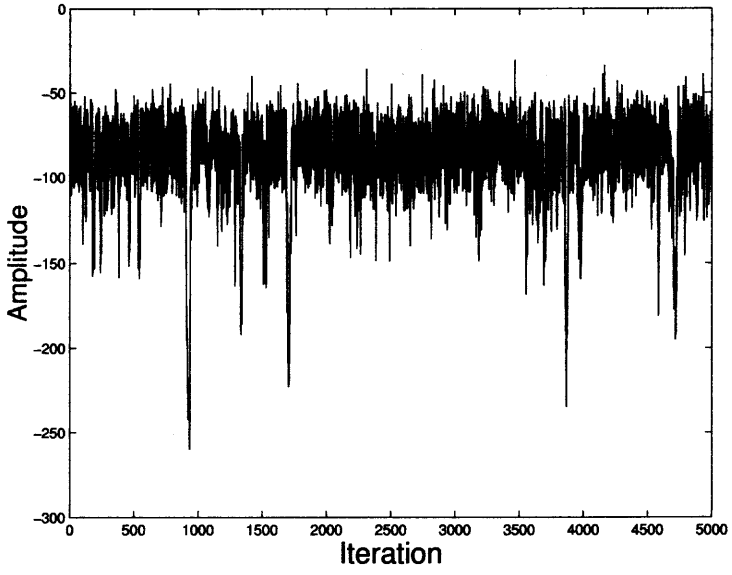

Figure 7.13 Samples obtained by Gibbs sampling for the amplitude of the second arrival vs. iteration. The correct amplitude is -80.

The amplitudes of the first, second, and third arrival are 100, -80 and 60, respectively. Table 7.4 shows the results for a single run consisting of 10,000 iterations.

As the table shows, divergent modes will eventually converge. The modes obtained for the amplitudes of the first two arrivals are diverging for the first 6000 iterations. However, after that point the modes obtained for all three amplitudes move towards the true values of the amplitudes.

Table 7.4 Monitoring the Modes of the Distribution

Iterations	A_1	A_2	A_3
1001-2000	455	-405	75
2001-3000	135	-125	75
3001-4000	395	-475	75
4001-5000	1175	-1175	75
5001-6000	1255	-1215	65
6001-7000	85	-75	65
7001-8000	95	-85	65
8001-9000	105	-85	65
9001-10000	95	-85	65

CHAPTER 8

APPLICATION TO REAL DATA

The Gibbs sampling algorithm presented here will now be applied to real data from the Haro Straight experiment. This experiment recorded signals obtained at several phones from an emitted sound. One of these signals is studied to estimate the number of arrivals, amplitude and time of each arrival, and the noise variance. For more details about the experiment the reader is referred to [5]. To test the performance of the algorithm, the received and transmitted signal are needed.

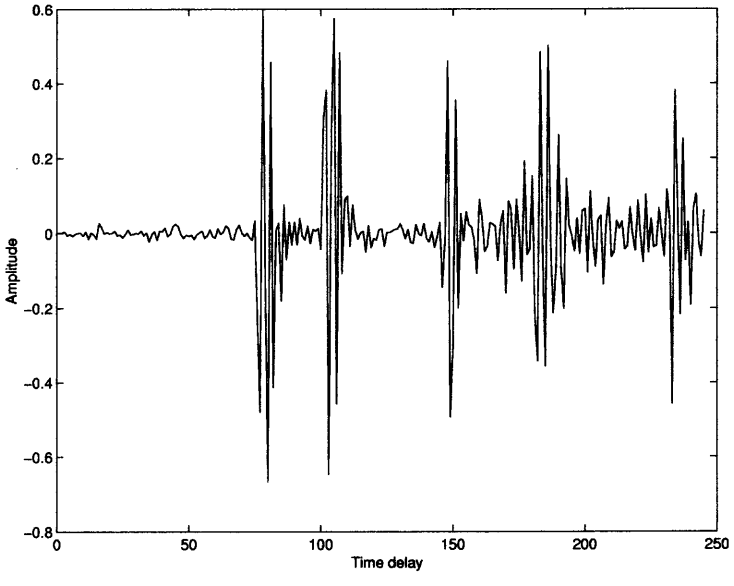

Figure 8.1 Real data from the Haro Straight experiment.

Although the received signal was available to us, we did not have access to the source (transmitted) signal. An estimate of the source signal was obtained by selecting one of the early arrivals from the received sequence. Figures 8.1 and 8.2 show the received signal and the estimate of the transmitted signal, respectively.

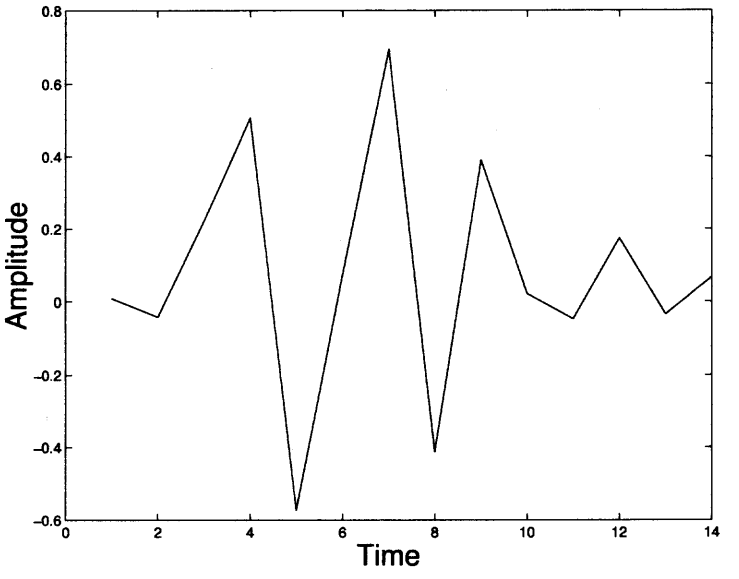

Figure 8.2 Transmitted signal for real data from the Haro Straight experiment.

The Gibbs sampler is run for several possible numbers of arrivals. Samples for the amplitudes are generated using Equation 3.7. Time delay samples are generated using Equation 3.9. Also acquired from the Gibbs sampling algorithm are samples for the noise variance using Equation 5.3. Clearly there are at least five arrivals present in Figure 8.1; thus estimates for signals with five, six, seven, and then eight arrivals are generated. Once the sampling process is complete, the modes of the distributions are found for each arrival. That is, since each arrival has an amplitude and time delay associated with it, the most frequently occurring pair is chosen as the estimate for the given arrival. Subsequently, the posterior distributions of the number of arrivals is attained. In Table 8.1 the estimates for the time delays and amplitudes are shown. Table 8.2 and Figure 8.3 contains the probability of a certain number of arrivals being present in the received signal.

Table 8.1 Estimates (Time Delay, Amplitude) Obtained for the Arrivals in the Real Data in Figure 8.1 Using Gibbs Sampling

	Assume 5 arrivals	Assume 6 arrivals	Assume 7 arrivals	Assume 8 arrivals
1st arrival	(74, -1.3)	(74, -1.3)	(74, -1.3)	(74, -1.3)
2nd arrival	(99, 1.1)	(99, 1.1)	(99, 1.1)	(99, 0.7)
3rd arrival	(144, -0.7)	(143, -0.5)	(143, -0.5)	(100, -1.0)
4th arrival	(179, -0.6)	(144,-0.9)	(144,-0.9)	(143,-0.5)
5th arrival	(227,-0.6)	(179, -0.8)	(179, -0.9)	(144, -0.9)
6th arrival		(230, -0.5)	(186, -0.4)	(179, -0.9)
7th arrival			(230,-0.6)	(186,-0.5)
8th arrival				(230,-0.6)

Studying the estimates in Table 8.1 and the probability associated with the various choices for the number of arrivals, one can infer that there are seven arrivals present in the data. Including a new arrival in the estimation process increases the probability until seven arrivals are considered. After that point, a reduction in probability is observed when additional arrivals are considered. Before concluding that the estimates for each arrival are those presented in Table 8.1 for the seven arrival case, convergence should be checked.

Table 8.2 Probability the Signal in Figure 8.1 Contains a Given Number of Arrivals

Number of arrivals	Probability
5	0.0761
6	0.2364
7	0.3999
8	0.2876

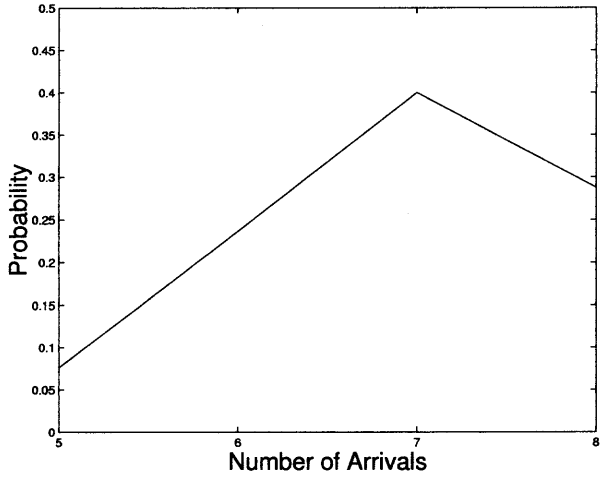

Figure 8.3 Probability the signal in Figure 8.1 contains a given number of arrivals.

Presented in Figure 8.4, are the samples obtained for the first time delay at each iteration from three different runs of the Gibbs sampling algorithm. Each run is quick to converge.

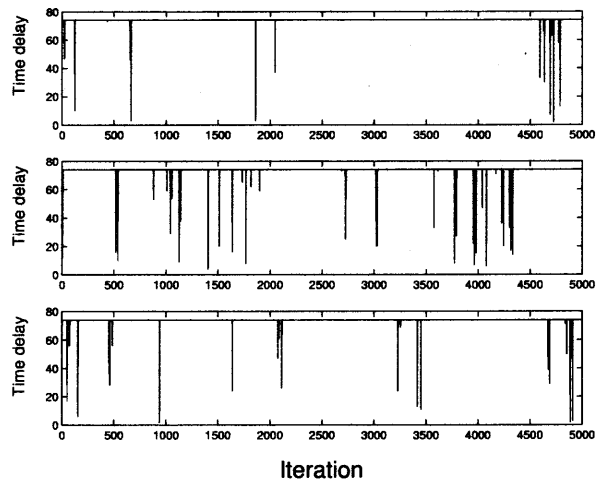

Figure 8.4 Samples for the first time delay from three runs of the Gibbs sampler.

Overall, the algorithm converged efficiently for each arrival. At this point, (74, -1.3), (99, 1.1), (143, -0.5), (144,-0.9), (179,-0.9), (186, -0.4), and (230,-0.6) are accepted as the time delays and amplitudes of the seven arrivals present in the Haro Straight data.

The only other component in the data to be estimated is the noise variance. The samples generated during the three runs of the Gibbs sampling algorithm are plotted in the histograms shown in Figure 8.5. In all three cases, the mode is at 0.005 and so we will assume that is the noise variance.

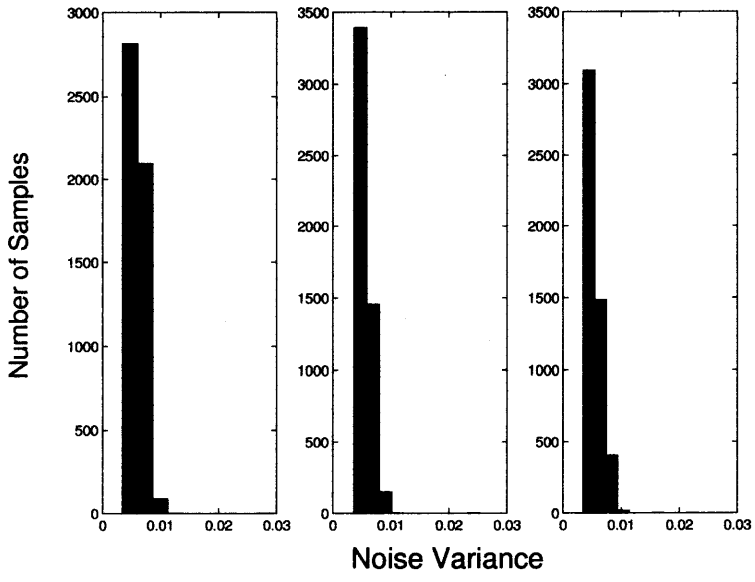

Figure 8.5 Samples for the variance from three different runs of the Gibbs sampler.

CHAPTER 9

CONCLUSIONS

In this work, an approach for the calculation of maximum a posteriori estimates for time delays, amplitudes, noise, and number of arrivals using a Gibbs sampling optimization method is developed. It has been shown that the approach is efficient to implement and can compute maximum a posteriori estimates rapidly in cases of several multi-paths, when the analytical maximum a posteriori approach is computationally not feasible.

The proposed Gibbs sampler was initially applied to synthetic data. Several cases were examined, testing the performance relative to the signal-to-noise ratio, number of multi-path arrivals, and time between the distinct arrivals. The results presented here have exhibited superiority to other optimization methods. The proposed method is faster than simulating annealing. It does not dependent on initial conditions like EM, and does not present any difficulties with closely spaced arrivals encountered with MF. In addition to efficiency and accuracy in the estimates, the Gibbs sampling method has the additional advantage of computing an estimate of the entire joint probability distribution of the unknown parameters, in contrast to most other methods that result only on point estimates, giving a more informative picture of the problem at hand.

The algorithm was also tested for convergence. This issue was approached in two different ways: First by checking parallel runs of the algorithm and then by examining the modes of the distribution. Convergence was typically attained within a relatively small number of iterations. On a few occasions, additional runs or iterations were necessary for the posterior distributions to stabilize.

The method was also applied to the Haro Straight data. Given a time series, the number of arrivals was recovered. Once this number was decided and the samples were checked for convergence, estimates were obtained for the time delays, amplitudes, and noise variance.

The work presented here can be further extended, treating the Gibbs sampler as the first step in a two step process. First, generate samples to determine values for the time delays, amplitudes, noise variance, and number of multi-paths. Once estimates are obtained for the parameters associated with the received signal, they can then be used to quickly find estimates for the parameters associated with the problem of interest, such as source and receiver location, sound speed profile, bottom properties, etc, in shallow water propagation.

BIBLIOGRAPHY

[1] A. Nehorai and S. Li, "An asymptotic maximum likelihood estimator for source parameters in a multipath environment," *IEEE*, pp. 2630–2633, 1988.

[2] J. Ianniello, "High-resolution multipath time delay estimation for broad-band random signals," *IEEE Transactions on Acoustics, Speech, and Signal Processing*, vol. 36, pp. 320–327, 1988.

[3] W. Hahn and S. Tretter, "Optimum processing for delay-vector estimation in passive signal arrays," *IEEE Transactions on Information Theory*, vol. 19, pp. 608–614, 1973.

[4] S. Dosso, M. Fallat, B. Sotirin, and J. Newton, "Array element localization for horizontal arrays via occam's inversion," *J. Acoust. Soc. Am.*, vol. 104, pp. 846–859, 1998.

[5] X. Ma, *Efficient Inversion Methods In Underwater Acoustics.* PhD thesis, New Jersey Institute of Technology, 2001.

[6] F. Jensen, W. Kuperman, M. Porter, and H. Schmidt, *Computational Ocean Acoustics.* New York: American Institute of Physics, 1994.

[7] M. B. Porter, "The KRAKEN normal mode program," *SACLANT Undersea Research Centre Memorandum (SM-245) and Naval Research Laboratory Mem. Rep. 6920*, 1991.

[8] A. Baggeroer, W. Kuperman, and P. N. Michalevsky, "An overview of matched field processing in ocean acoustics," *IEEE Journal of Oceanic Engineering*, vol. 18, pp. 401–424, 1993.

[9] A. Tolstoy, *Matched Field Processing for Underwater Acoustics.* Singapore: World Scientific, 1993.

[10] M. D. Collins and W. Kuperman, "Focalization: Environmental focusing and source localization," *J. Acoust. Soc. Am.*, pp. 1410–1422, 1991.

[11] J. F. Smith and S. Finette, "Simulated annealing as a method of deconvolution for acoustic transients measured on a vertical array," *J. Acoust. Soc. Am.*, pp. 2315–2325, 1993.

[12] M. Feder and E. Weinstein, "Parameter estimation of superimposed signals using the EM algorithm," *IEEE Transactions on Acoustics, Speech, and Signal Processing*, vol. 36, pp. 477–489, 1988.

[13] A. Blackowiak and S. Rajan, "Multi-path arrival estimates using simulated annealing; application to crosshole tomography experiment," *IEEE Journal of Oceanic Engineering*, pp. 157–165, 1995.

[14] L. Jaschke and N. Chapman, "Matched field inversion of broadband data using the freeze bath method." Submitted to J. Acoust. Soc. Am., 1998.

[15] P. Pignot and R. Chapman, "Tomographic inversion for geoacoustic properties in a range dependent shallow water evvironment." Submitted to J. Acoust. Soc. Am., 1998.

[16] J. Ehrenberg, T. Ewart, and R. Morris, "Signal-processing techniques for resolving individual pulses in a multipath signal," *J. Acoust. Soc. Am.*, pp. 1861–1865, 1978.

[17] R. J. Vaccaro and R. L. Field, "Transient signal extraction in a multipath environment," *IEEE*, pp. 115–120, 1990.

[18] T. G. Manickam, R. J. Vaccaro, and D. W. Tufts, "A least-squares algorithm for multipath time-delay estimation," *IEEE Transactions on Signal Processing*, vol. 42, pp. 3229–3233, 1994.

[19] L. Jaschke, "Geophysical inversion by the freeze bath method with an application to geoacoustic ocean bottom parameter estimation," Master's thesis, School of Earth and Ocean Science, 1997.

[20] G. J. McLachlan and T. Krishnan, *The EM Algorithm and Extensions.* New York, NY: John Wiley Sons, Inc., 1997.

[21] I. Ziskind and M. Wax, "Maximum likelihood localization of multiple sources by alternating projection," *IEEE Transactions on Acoustics, Speech, and Signal Processing*, vol. 36, pp. 1553–1560, 1988.

[22] M. Feder and E. Weinstein, "An EM algorithm for multisensor tdoa/dd estimation in a multipath propagation environment," *IEEE*, pp. 3117–3120, 1996.

[23] M. Sen, P. L. Stoffa, and H. Schmidt, *Global Optimization Methods in Geophysical Inversion.* Elsevier, 1995.

[24] W. R. Gilks, S. Richardson, and D. J. Spiegelhalter, *Markov Chain Monte Carlo in Practice.* Chapman and Hall/CRC, 1996.

[25] A. E. Gelfand, A. F. M. Smith, and T.-M. Lee, "Bayesian analysis of constrained parameter and truncated data problems using gibbs sampling," *Journal of the Americal Statistical Association*, vol. 87, pp. 523–532, 1992.

[26] S. Geman and D. Geman, "Stochastic relaxation, gibbs distributions, and the bayesian restoration of images," *IEEE Transactions on Pattern Analysis and Machine Intelligence*, pp. 721–741, 1984.

[27] A. Gelfand, S. Hills, A. Racine-Poon, and A. Smith, "Illustration of bayesian inference in normal data models using gibbs sampling," *Journal of the American Statistical Association*, vol. 85, pp. 972–985, 1990.

[28] G. Casella and E. I. George, "Explaining the gibbs sampler," *The American Statistician*, vol. 46, pp. 167–174, 1992.

[29] A. Whalen, *Detection of Signals in Noise.* California: Academic Press, Inc., 1971.

[30] S. M. Ross, *Introduction To Probability Models.* Academy Press, 1997.

[31] R. Hogg and E. Tanis, *Probability and Statistical Inference.* Macmillan, 1993.

[32] Z.-H. Michalopoulou, X. Ma, M. Picarelli, and U. Ghosh-Dastidar, "Fast matching methods for inversion with underwater sound," in *Proceedings of Ocean 2000*, (Rhode Island), 2000.

[33] A. Tolstoy, N. R. Chapman, and G. Brooke, "Workshop '97: Benchmarking for geoacoustic inversion in shallow water," *Journal of Computational Acoustics*, vol. 6, pp. 1–28, 1998.

[34] G. Box and G. Tiao, *Bayesian Inference in Statistical Analysis.* Philippines: Addison-Wesley Publishing Company, Inc., 1973.

[35] R. Vaccaro, C. Ramalingam, and D. Tufts, "Least-squares time-delay estimation for transient signals in a multipath environment," *J. Acoust. Soc. Am.*, vol. 92, pp. 210–218, 1992.

[36] M. Wax and T. Kailath, "Detection of signals by information theoretic criteria," *IEEE Transactions on Acoustics, Speech, and Signal Processing*, vol. 33, pp. 387–392, 1985.